Cell-Free Massive MIMO Versus Small Cells

Cell-Free Massive MIMO versus Small Cells

Hien Quoc Ngo, Alexei Ashikhmin, Hong Yang, Erik G. Larsson, and Thomas L. Marzetta

Abstract—A Cell-Free Massive MIMO (multiple-input multiple-output) system comprises a very large number of distributed access points (APs) which simultaneously serve a much smaller number of users over the same time/frequency resources based on directly measured channel characteristics. The APs and users have only one antenna each. The APs acquire channel state information through time-division duplex operation and the reception of uplink pilot signals transmitted by the users. The APs perform multiplexing/de-multiplexing through conjugate beamforming on the downlink and matched filtering on the uplink. Closed-form expressions for individual user uplink and downlink throughputs lead to max-min power control algorithms. Max-min power control ensures uniformly good service throughout the area of coverage. A pilot assignment algorithm helps to mitigate the effects of pilot contamination, but power control is far more important in that regard.

Cell-Free Massive MIMO has considerably improved performance with respect to a conventional small-cell scheme, whereby each user is served by a dedicated AP, in terms of both 95%-likely per-user throughput and immunity to shadow fading spatial correlation. Under uncorrelated shadow fading conditions, the cell-free scheme provides nearly 5-fold improvement in 95%-likely per-user throughput over the small-cell scheme, and 10-fold improvement when shadow fading is correlated.

Index Terms—Cell-Free Massive MIMO system, conjugate beamforming, Massive MIMO, network MIMO, small cell.

I. INTRODUCTION

MASSIVE multiple-input multiple-output (MIMO), where a base station with many antennas simultaneously serves many users in the same time-frequency resource, is a promising 5G wireless access technology that can provide high throughput, reliability, and energy efficiency with simple signal processing [2], [3]. Massive antenna arrays at the base stations can be deployed in collocated or distributed setups. Collocated Massive MIMO architectures, where all service antennas are located in a compact area, have the advantage of low backhaul requirements. In contrast, in distributed Massive MIMO systems, the service antennas are spread out over a large area. Owing to their ability to more efficiently exploit diversity against the shadow fading, distributed systems can potentially offer much higher probability of coverage than collocated Massive MIMO [4], at the cost of increased backhaul requirements.

In this work, we consider a distributed Massive MIMO system where a large number of service antennas, called access points (APs), serve a much smaller number of autonomous users distributed over a wide area [1]. All APs cooperate phase-coherently via a backhaul network, and serve all users in the same time-frequency resource via time-division duplex (TDD) operation. There are no cells or cell boundaries. Therefore, we call this system "Cell-Free Massive MIMO". Since Cell-Free Massive MIMO combines the distributed MIMO and Massive MIMO concepts, it is expected to reap all benefits from these two systems. In addition, since the users now are close to the APs, Cell-Free Massive MIMO can offer a high coverage probability. Conjugate beamforming/matched filtering techniques, also known as maximum-ratio processing, are used both on uplink and downlink. These techniques are computationally simple and can be implemented in a distributed manner, that is, with most processing done locally at the APs.[1]

In Cell-Free Massive MIMO, there is a central processing unit (CPU), but the information exchange between the APs and this CPU is limited to the payload data, and power control coefficients that change slowly. There is no sharing of instantaneous channel state information (CSI) among the APs or the central unit. All channels are estimated at the APs through uplink pilots. The so-obtained channel estimates are used to precode the transmitted data in the downlink and to perform data detection in the uplink. Throughout we emphasize per-user throughput rather than sum-throughput. To that end we employ max-min power control.

In principle, Cell-Free Massive MIMO is an incarnation of general ideas known as "virtual MIMO", "network MIMO", "distributed MIMO", "(coherent) cooperative multipoint joint processing" (CoMP) and "distributed antenna systems" (DAS). The objective is to use advanced backhaul to achieve coherent processing across geographically distributed base station antennas, in order to provide uniformly good service for all users in the network. The outstanding aspect of Cell-Free Massive MIMO is its operating regime: many single-antenna access points simultaneously serve a much smaller number of users, using computationally simple (conjugate beamforming) signal processing. This facilitates the exploitation of phenomena such as favorable propagation and channel hardening – which are

H. Q. Ngo and E. G. Larsson are with the Department of Electrical Engineering (ISY), Linköping University, 581 83 Linköping, Sweden (Email: hien.ngo@liu.se; erik.g.larsson@liu.se). H. Q. Ngo is also with the School of Electronics, Electrical Engineering and Computer Science, Queen's University Belfast, Belfast BT3 9DT, U.K.

A. Ashikhmin, H. Yang and T. L. Marzetta are with Nokia Bell Laboratories, Murray Hill, NJ 07974 USA (Email: alexei.ashikhmin@nokia-bell-labs.com; h.yang@nokia-bell-labs.com; tom.marzetta@nokia-bell-labs.com).

---

[1]Other linear processing techniques (e.g. zero-forcing) may improve the system performance, but they require more backhaul than maximum-ratio processing does. The tradeoff between the implementation complexity and the system performance for these techniques is of interest and needs to be studied in future work.

also key characteristics of cellular Massive MIMO [5]. In turn, this enables the use of computationally efficient and globally optimal algorithms for power control, and simple schemes for pilot assignment (as shown later in this paper). In summary, Cell-Free Massive MIMO is a useful and scalable implementation of the network MIMO and DAS concepts – much in the same way as cellular Massive MIMO is a useful and scalable form of the original multiuser MIMO concept (see, e.g., [5, Chap. 1] for an extended discussion of the latter).

Related work:

Many papers have studied network MIMO [6], [8], [9] and DAS [7], [10], [11], and indicated that network MIMO and DAS may offer higher rates than colocated MIMO. However, these works did not consider the case of very large numbers of service antennas. Related works which use a similar system model as in our paper are [12]–[18]. In these works, DAS with the use of many antennas, called large-scale DAS or distributed massive MIMO, was exploited. However, in all those papers, perfect CSI was assumed at both the APs and the users, and in addition, the analysis in [18] was asymptotic in the number of antennas and the number of users. A realistic analysis must account for imperfect CSI, which is an inevitable consequence of the finite channel coherence in a mobile system and which typically limits the performance of any wireless system severely [19]. Large-scale DAS with imperfect CSI was considered in [20]–[23] for the special case of orthogonal pilots or the reuse of orthogonal pilots, and in [24] assuming frequency-division duplex (FDD) operation. In addition, in [20], the authors exploited the low-rank structure of users' channel covariance matrices, and examined the performance of uplink transmission with matched-filtering detection, under the assumption that all users use the same pilot sequence. By contrast, in the current paper, we assume TDD operation, hence rely on reciprocity to acquire CSI, and we assume the use of arbitrary pilot sequences in the network – resulting in pilot contamination, which was not studied in previous work. We derive rigorous capacity lower bounds valid for any finite number of APs and users, and give algorithms for optimal power control (to global optimality) and pilot assignment.

The papers cited above compare the performance between distributed and collocated Massive MIMO systems. An alternative to (distributed) MIMO systems is to deploy small cells, consisting of APs that do not cooperate. Small-cell systems are considerably simpler than Cell-Free Massive MIMO, since only data and power control coefficients are exchanged between the CPU and the APs. It is expected that Cell-Free Massive MIMO systems perform better than small-cell systems. However it is not clear, quantitatively, how much Cell-Free Massive MIMO systems can gain compared to small-cell systems. Most previous work compares collocated Massive MIMO and small-cell systems [25], [26]. In [25], the authors show that, when the number of cells is large, a small-cell system is more energy-efficient than a collocated Massive MIMO system. By taking into account a specific transceiver hardware impairment and power consumption model, paper [26] shows that reducing the cell size (or increasing the base station density) is the way to increase the energy efficiency. However when the circuit power dominates over the transmission power,

this benefit saturates. Energy efficiency comparisons between collocated massive MIMO and small-cell systems are also studied in [27], [28]. There has however been little work that compares distributed Massive MIMO and small-cell systems. A comparison between small-cell and distributed Massive MIMO systems is reported in [12], assuming perfect CSI at both the APs and the users. Yet, a comprehensive performance comparison between small-cell and distributed Massive MIMO systems that takes into account the effects of imperfect CSI, pilot assignment, and power control is not available in the existing literature.

Specific contributions of the paper:

- We consider a cell-free massive MIMO with conjugate beamforming on the downlink and matched filtering on the uplink. We show that, as in the case of collocated systems, when the number of APs goes to infinity, the effects of non-coherent interference, small-scale fading, and noise disappear.
- We derive rigorous closed-form capacity lower bounds for the Cell-Free Massive MIMO downlink and uplink with finite numbers of APs and users. Our analysis takes into account the effects of channel estimation errors, power control, and non-orthogonality of pilot sequences.
- We compare two pilot assignment schemes: *random assignment* and *greedy assignment*.
- We devise max-min fairness power control algorithms that maximize the smallest of all user rates. Globally optimal solutions can be computed by solving a sequence of second-order cone programs (SOCPs) for the downlink, and a sequence of linear programs for the uplink.
- We quantitatively compare the performance of Cell-Free Massive MIMO to that of small-cell systems, under uncorrelated and correlated shadow fading models.

The rest of paper is organized as follows. In Section II, we describe the Cell-Free Massive MIMO system model. In Section III, we present the achievable downlink and uplink rates. The pilot assignment and power control schemes are developed in Section IV. The small-cell system is discussed in Section V. We provide numerical results and discussions in Section VI and finally conclude the paper in Section VII.

Notation: Boldface letters denote column vectors. The superscripts $()^*$, $()^T$, and $()^H$ stand for the conjugate, transpose, and conjugate-transpose, respectively. The Euclidean norm and the expectation operators are denoted by $\| \cdot \|$ and $\mathbb{E}\{\cdot\}$, respectively. Finally, $z \sim \mathcal{CN}\left(0, \sigma^2\right)$ denotes a circularly symmetric complex Gaussian random variable (RV) z with zero mean and variance σ^2, and $z \sim \mathcal{N}(0, \sigma^2)$ denotes a real-valued Gaussian RV.

II. CELL-FREE MASSIVE MIMO SYSTEM MODEL

We consider a Cell-Free Massive MIMO system with M APs and K users. All APs and users are equipped with a single antenna, and they are randomly located in a large area. Furthermore, all APs connect to a central processing unit via a backhaul network, see Figure 1. We assume that all M APs simultaneously serve all K users in the same time-frequency resource. The transmission from the APs to the users (downlink transmission) and the transmission from the users to the
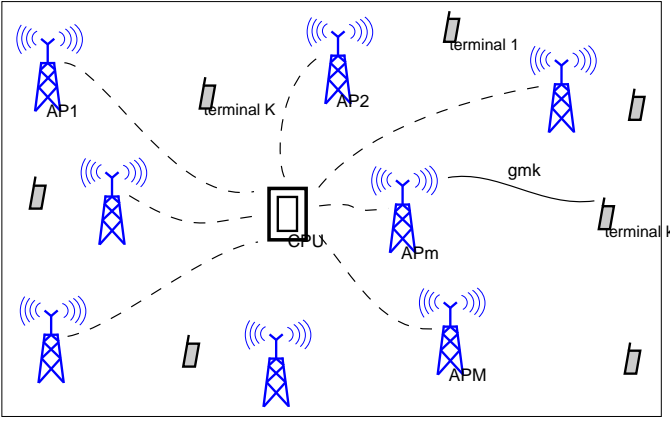
Fig. 1. Cell-Free Massive MIMO system.

APs (uplink transmission) proceed by TDD operation. Each coherence interval is divided into three phases: uplink training, downlink payload data transmission, and uplink payload data transmission. In the uplink training phase, the users send pilot sequences to the APs and each AP estimates the channel to all users. The so-obtained channel estimates are used to precode the transmit signals in the downlink, and to detect the signals transmitted from the users in the uplink. In this work, to avoid sharing of channel state information between the APs, we consider conjugate beamforming in the downlink and matched filtering in the uplink.

No pilots are transmitted in the downlink of Cell-Free Massive MIMO. The users do not need to estimate their effective channel gain, but instead rely on channel hardening, which makes this gain close to its expected value, a known deterministic constant. Our capacity bounds account for the error incurred when the users use the average effective channel gain instead of the actual effective gain. Channel hardening in Massive MIMO is discussed, for example, in [2].

Notation is adopted and assumptions are made as follows:

- The channel model incorporates the effects of small-scale fading and large-scale fading (that latter includes path loss and shadowing). The small-scale fading is assumed to be static during each coherence interval, and change independently from one coherence interval to the next. The large-scale fading changes much more slowly, and stays constant for several coherence intervals. Depending on the user mobility, the large-scale fading may stay constant for a duration of at least some 40 small-scale fading coherence intervals [29], [30].
- We assume that the channel is reciprocal, i.e., the channel gains on the uplink and on the downlink are the same. This reciprocity assumption requires TDD operation and perfect calibration of the hardware chains. The feasibility of the latter is demonstrated for example in [31] for collocated Massive MIMO and it is conceivable that the problem can be similarly somehow for Cell-Free Massive MIMO. Investigating the effect of imperfect calibration is an important topic for future work.
- We let g_{mk} denote the channel coefficient between the

kth user and the mth AP. The channel g_{mk} is modelled as follows:

$$g_{mk} = \beta_{mk}^{1/2} h_{mk}, \tag{1}$$

where h_{mk} represents the small-scale fading, and β_{mk} represents the large-scale fading. We assume that h_{mk}, $m = 1, \ldots, M$, $K = 1, \ldots K$, are independent and identically distributed (i.i.d.) $\mathcal{CN}(0, 1)$ RVs. The justification of the assumption of independent small-scale fading is that the APs and the users are distributed over a wide area, and hence, the set of scatterers is likely to be different for each AP and each user.

- We assume that all APs are connected via perfect backhaul that offers error-free and infinite capacity to the CPU. In practice, backhaul will be subject to significant practical constraints [32], [33]. Future work is needed to quantify the impact of backhaul constraints on performance.
- In all scenarios, we let q_k denote the symbol associated with the kth user. These symbols are mutually independent, and independent of all noise and channel coefficients.

A. Uplink Training

The Cell-Free Massive MIMO system employs a wide spectral bandwidth, and the quantities g_{mk} and h_{mk} are dependent on frequency; however β_{mk} is constant with respect to frequency. The propagation channels are assumed to be piecewise constant over a coherence time interval and a frequency coherence interval. It is necessary to perform training within each such time/frequency coherence block. We assume that β_{mk} is known, a priori, wherever required.

Let τ_c be the length of the coherence interval (in samples), which is equal to the product of the coherence time and the coherence bandwidth, and let τ^{cf} be the uplink training duration (in samples) per coherence interval, where the superscript cf stands for "cell-free". It is required that $\tau^{cf} < \tau_c$. During the training phase, all K users simultaneously send pilot sequences of length τ^{cf} samples to the APs. Let $\sqrt{\tau^{cf}}\boldsymbol{\varphi}_k \in \mathbb{C}^{\tau^{cf} \times 1}$, where $\|\boldsymbol{\varphi}_k\|^2 = 1$, be the pilot sequence used by the kth user, $k = 1, 2, \cdots, K$. Then, the $\tau^{cf} \times 1$ received pilot vector at the mth AP is given by

$$\mathbf{y}_{p,m} = \sqrt{\tau^{cf}\rho_p^{cf}} \sum_{k=1}^{K} g_{mk}\boldsymbol{\varphi}_k + \mathbf{w}_{p,m}, \tag{2}$$

where ρ_p^{cf} is the normalized signal-to-noise ratio (SNR) of each pilot symbol and $\mathbf{w}_{p,m}$ is a vector of additive noise at the mth AP. The elements of $\mathbf{w}_{p,m}$ are i.i.d. $\mathcal{CN}(0, 1)$ RVs.

Based on the received pilot signal $\mathbf{y}_{p,m}$, the mth AP estimates the channel $g_{mk}, k = 1, ..., K$. Denote by $\breve{y}_{p,mk}$ the projection of $\mathbf{y}_{p,m}$ onto $\boldsymbol{\varphi}_k^H$:

$$\breve{y}_{p,mk} = \boldsymbol{\varphi}_k^H \mathbf{y}_{p,m}$$

$$= \sqrt{\tau^{cf}\rho_p^{cf}} g_{mk} + \sqrt{\tau^{cf}\rho_p^{cf}} \sum_{k' \neq k}^{K} g_{mk'}\boldsymbol{\varphi}_k^H \boldsymbol{\varphi}_{k'} + \boldsymbol{\varphi}_k^H \mathbf{w}_{p,m}. \tag{3}$$

Although, for arbitrary pilot sequences, $\check{y}_{\mathrm{p},mk}$ is not a sufficient statistic for the estimation of g_{mk}, one can still use this quantity to obtain suboptimal estimates. In the special case when any two pilot sequences are either identical or orthogonal, then $\check{y}_{\mathrm{p},mk}$ is a sufficient statistic, and estimates based on $\check{y}_{\mathrm{p},mk}$ are optimal. The MMSE estimate of g_{mk} given $\check{y}_{\mathrm{p},mk}$ is

$$\hat{g}_{mk} = \frac{\mathbb{E}\left\{\check{y}_{\mathrm{p},mk}^* g_{mk}\right\}}{\mathbb{E}\left\{|\check{y}_{\mathrm{p},mk}|^2\right\}} \check{y}_{\mathrm{p},mk} = c_{mk}\check{y}_{\mathrm{p},mk}, \qquad (4)$$

where

$$c_{mk} \triangleq \frac{\sqrt{\tau^{\mathrm{cf}}\rho_{\mathrm{p}}^{\mathrm{cf}}}\beta_{mk}}{\tau^{\mathrm{cf}}\rho_{\mathrm{p}}^{\mathrm{cf}}\sum_{k'=1}^{K}\beta_{mk'}\left|\boldsymbol{\varphi}_k^H\boldsymbol{\varphi}_{k'}\right|^2 + 1}.$$

Remark 1: If $\tau^{\mathrm{cf}} \geq K$, then we can choose $\boldsymbol{\varphi}_1, \boldsymbol{\varphi}_2, \cdots, \boldsymbol{\varphi}_K$ so that they are pairwisely orthogonal, and hence, the second term in (3) disappears. Then the channel estimate $\hat{g}_{mk}$ is independent of $g_{mk'}$, $k' \neq k$. However, owing to the limited length of the coherence interval, in general, $\tau^{\mathrm{cf}} < K$, and mutually non-orthogonal pilot sequences must be used throughout the network. The channel estimate $\hat{g}_{mk}$ is degraded by pilot signals transmitted from other users, owing to the second term in (3). This causes the so-called pilot contamination effect.

Remark 2: The channel estimation is performed in a decentralized fashion. Each AP autonomously estimates the channels to the K users. The APs do not cooperate on the channel estimation, and no channel estimates are interchanged among the APs.

B. Downlink Payload Data Transmission

The APs treat the channel estimates as the true channels, and use conjugate beamforming to transmit signals to the K users. The transmitted signal from the mth AP is given by

$$x_m = \sqrt{\rho_{\mathrm{d}}^{\mathrm{cf}}}\sum_{k=1}^{K}\eta_{mk}^{1/2}\hat{g}_{mk}^* q_k, \qquad (5)$$

where q_k, which satisfies $\mathbb{E}\left\{|q_k|^2\right\} = 1$, is the symbol intended for the kth user, and η_{mk}, $m = 1,\ldots,M$, $k = 1,\ldots K$, are power control coefficients chosen to satisfy the following power constraint at each AP:

$$\mathbb{E}\left\{|x_m|^2\right\} \leq \rho_{\mathrm{d}}^{\mathrm{cf}}. \qquad (6)$$

With the channel model in (1), the power constraint $\mathbb{E}\left\{|x_m|^2\right\} \leq \rho_{\mathrm{d}}^{\mathrm{cf}}$ can be rewritten as:

$$\sum_{k=1}^{K}\eta_{mk}\gamma_{mk} \leq 1, \quad \text{for all } m, \qquad (7)$$

where

$$\gamma_{mk} \triangleq \mathbb{E}\left\{|\hat{g}_{mk}|^2\right\} = \sqrt{\tau^{\mathrm{cf}}\rho_{\mathrm{p}}^{\mathrm{cf}}}\beta_{mk}c_{mk}. \qquad (8)$$

The received signal at the kth user is given by

$$\begin{aligned} r_{\mathrm{d},k} &= \sum_{m=1}^{M}g_{mk}x_m + w_{\mathrm{d},k} \\ &= \sqrt{\rho_{\mathrm{d}}^{\mathrm{cf}}}\sum_{m=1}^{M}\sum_{k'=1}^{K}\eta_{mk'}^{1/2}g_{mk}\hat{g}_{mk'}^* q_{k'} + w_{\mathrm{d},k}, \qquad (9) \end{aligned}$$

where $w_{\mathrm{d},k}$ is additive $\mathcal{CN}(0,1)$ noise at the kth user. Then q_k will be detected from $r_{\mathrm{d},k}$.

C. Uplink Payload Data Transmission

In the uplink, all K users simultaneously send their data to the APs. Before sending the data, the kth user weights its symbol q_k, $\mathbb{E}\left\{|q_k|^2\right\} = 1$, by a power control coefficient $\sqrt{\eta_k}$, $0 \leq \eta_k \leq 1$. The received signal at the mth AP is given by

$$y_{\mathrm{u},m} = \sqrt{\rho_{\mathrm{u}}^{\mathrm{cf}}}\sum_{k=1}^{K}g_{mk}\sqrt{\eta_k}q_k + w_{\mathrm{u},m}, \qquad (10)$$

where $\rho_{\mathrm{u}}^{\mathrm{cf}}$ is the normalized uplink SNR and $w_{\mathrm{u},m}$ is additive noise at the mth AP. We assume that $w_{\mathrm{u},m} \sim \mathcal{CN}(0,1)$.

To detect the symbol transmitted from the kth user, q_k, the mth AP multiplies the received signal $y_{\mathrm{u},m}$ with the conjugate of its (locally obtained) channel estimate $\hat{g}_{mk}$. Then the so-obtained quantity $\hat{g}_{mk}^* y_{\mathrm{u},m}$ is sent to the CPU via a backhaul network. The CPU sees

$$\begin{aligned} r_{\mathrm{u},k} &= \sum_{m=1}^{M}\hat{g}_{mk}^* y_{\mathrm{u},m} \\ &= \sum_{k'=1}^{K}\sum_{m=1}^{M}\sqrt{\rho_{\mathrm{u}}^{\mathrm{cf}}\eta_{k'}}\hat{g}_{mk}^* g_{mk'}q_{k'} + \sum_{m=1}^{M}\hat{g}_{mk}^* w_{\mathrm{u},m}. \quad (11) \end{aligned}$$

Then, q_k is detected from $r_{\mathrm{u},k}$.

III. PERFORMANCE ANALYSIS

A. Large-M Analysis

In this section, we provide some insights into the performance of Cell-Free Massive MIMO systems when M is very large. The convergence analysis is done conditioned on a set of deterministic large-scale fading coefficients $\{\beta_{mk}\}$. We show that, as in the case of Collocated Massive MIMO, when $M \to \infty$, the channels between the users and the APs become orthogonal. Therefore, with conjugate beamforming respectively matched filtering, non-coherent interference, small-scale fading, and noise disappear. The only remaining impairment is pilot contamination, which consists of interference from users using same pilot sequences as the user of interest in the training phase.

On downlink, from (9), the received signal at the kth user can be written as:

$$\begin{aligned} r_{\mathrm{d},k} &= \underbrace{\sqrt{\rho_{\mathrm{d}}^{\mathrm{cf}}}\sum_{m=1}^{M}\eta_{mk}^{1/2}g_{mk}\hat{g}_{mk}^* q_k}_{\mathrm{DS}_k} \\ &\quad + \underbrace{\sqrt{\rho_{\mathrm{d}}^{\mathrm{cf}}}\sum_{m=1}^{M}\sum_{k'\neq k}^{K}\eta_{mk'}^{1/2}g_{mk}\hat{g}_{mk'}^* q_{k'}}_{\mathrm{MUI}_k} + w_{\mathrm{d},k}, \qquad (12) \end{aligned}$$

where DS_k and MUI_k represent the desired signal and multiuser interference, respectively.

By using the channel estimates in (4), we have

$$
\sum_{m=1}^{M} \eta_{mk'}^{1/2} g_{mk} \hat{g}_{mk'}^*
$$

$$
= \sum_{m=1}^{M} \eta_{mk'}^{1/2} c_{mk'} g_{mk} \left(\sqrt{\tau^{\mathrm{cf}} \rho_{\mathrm{p}}^{\mathrm{cf}}} \sum_{k''=1}^{K} g_{mk''} \boldsymbol{\varphi}_{k'}^H \boldsymbol{\varphi}_{k''} + \tilde{w}_{\mathrm{p},mk'} \right)^*
$$

$$
= \sqrt{\tau^{\mathrm{cf}} \rho_{\mathrm{p}}^{\mathrm{cf}}} \sum_{m=1}^{M} \eta_{mk'}^{1/2} c_{mk'} |g_{mk}|^2 \boldsymbol{\varphi}_{k'}^T \boldsymbol{\varphi}_k^*
$$

$$
+ \sqrt{\tau^{\mathrm{cf}} \rho_{\mathrm{p}}^{\mathrm{cf}}} \sum_{k''\neq k}^{K} \sum_{m=1}^{M} \eta_{mk'}^{1/2} c_{mk'} g_{mk} g_{mk''}^* \boldsymbol{\varphi}_{k'}^T \boldsymbol{\varphi}_{k''}^*
$$

$$
+ \sum_{m=1}^{M} \eta_{mk'}^{1/2} c_{mk'} g_{mk} \tilde{w}_{\mathrm{p},mk'}^*, \tag{13}
$$

where $\tilde{w}_{\mathrm{p},mk'} \triangleq \boldsymbol{\varphi}_{k'}^H \mathbf{w}_{\mathrm{p},m}$. Then by Tchebyshev's theorem [34],[2] we have

$$
\frac{1}{M} \sum_{m=1}^{M} \eta_{mk'}^{1/2} g_{mk} \hat{g}_{mk'}^* - \frac{1}{M} \sqrt{\tau^{\mathrm{cf}} \rho_{\mathrm{p}}^{\mathrm{cf}}} \sum_{m=1}^{M} \eta_{mk'}^{1/2} c_{mk'} \beta_{mk} \boldsymbol{\varphi}_{k'}^T \boldsymbol{\varphi}_k^*
$$

$$
\xrightarrow[M\to\infty]{P} 0. \tag{14}
$$

Using (14), we obtain the following results:

$$
\frac{1}{M} \mathrm{DS}_k - \frac{1}{M} \sqrt{\tau^{\mathrm{cf}} \rho_{\mathrm{p}}^{\mathrm{cf}} \rho_{\mathrm{d}}^{\mathrm{cf}}} \sum_{m=1}^{M} \eta_{mk}^{1/2} c_{mk} \beta_{mk} q_k \xrightarrow[M\to\infty]{P} 0, \tag{15}
$$

$$
\frac{1}{M} \mathrm{MUI}_k - \frac{1}{M} \sqrt{\tau^{\mathrm{cf}} \rho_{\mathrm{p}}^{\mathrm{cf}} \rho_{\mathrm{d}}^{\mathrm{cf}}} \sum_{m=1}^{M} \sum_{k'\neq k}^{K} \eta_{mk'}^{1/2} c_{mk'} \beta_{mk} \boldsymbol{\varphi}_{k'}^T \boldsymbol{\varphi}_k^* q_{k'}
$$

$$
\xrightarrow[M\to\infty]{P} 0. \tag{16}
$$

The above expressions show that when $M \to \infty$, the received signal includes only the desired signal plus interference originating from the pilot sequence non-orthogonality:

$$
\frac{r_{\mathrm{d},k}}{M} - \frac{\sqrt{\tau^{\mathrm{cf}} \rho_{\mathrm{p}}^{\mathrm{cf}} \rho_{\mathrm{d}}^{\mathrm{cf}}}}{M} \left(\sum_{m=1}^{M} \eta_{mk}^{1/2} c_{mk} \beta_{mk} q_k \right.
$$

$$
\left. + \sum_{m=1}^{M} \sum_{k'\neq k}^{K} \eta_{mk'}^{1/2} c_{mk'} \beta_{mk} \boldsymbol{\varphi}_{k'}^T \boldsymbol{\varphi}_k^* q_{k'} \right) \xrightarrow[M\to\infty]{P} 0. \tag{17}
$$

If the pilot sequences are pairwisely orthogonal, i.e., $\boldsymbol{\varphi}_{k'}^H \boldsymbol{\varphi}_k = 0$ for $k \neq k'$, then the received signal becomes free of interference and noise:

$$
\frac{r_{\mathrm{d},k}}{M} - \frac{\sqrt{\tau^{\mathrm{cf}} \rho_{\mathrm{p}}^{\mathrm{cf}} \rho_{\mathrm{d}}^{\mathrm{cf}}}}{M} \sum_{m=1}^{M} \eta_{mk}^{1/2} c_{mk} \beta_{mk} q_k \xrightarrow[M\to\infty]{P} 0. \tag{18}
$$

Similar results hold on the uplink.

---

[2]Tchebyshev's theorem: Let $X_1, X_2, ... X_n$ be independent RVs such that $\mathbb{E}\{X_i\} = \mu_i$ and $\mathrm{Var}\{X_i\} \leq c < \infty, \forall i$. Then

$$
\frac{1}{n}(X_1 + X_2 + ... + X_n) - \frac{1}{n}(\mu_1 + \mu_2 + ... \mu_n) \xrightarrow{P} 0.
$$

B. Achievable Rate for Finite M

In this section, we derive closed-form expressions for the downlink and uplink achievable rates, using the analysis technique from [21], [35].

1) Achievable Downlink Rate: We assume that each user has knowledge of the channel statistics but not of the channel realizations. The received signal $r_{\mathrm{d},k}$ in (9) can be written as

$$
r_{\mathrm{d},k} = \mathrm{DS}_k \cdot q_k + \mathrm{BU}_k \cdot q_k + \sum_{k'\neq k}^{K} \mathrm{UI}_{kk'} \cdot q_{k'} + w_{\mathrm{d},k}, \tag{19}
$$

where

$$
\mathrm{DS}_k \triangleq \sqrt{\rho_{\mathrm{d}}^{\mathrm{cf}}} \, \mathbb{E}\left\{ \sum_{m=1}^{M} \eta_{mk}^{1/2} g_{mk} \hat{g}_{mk}^* \right\}, \tag{20}
$$

$$
\mathrm{BU}_k \triangleq \sqrt{\rho_{\mathrm{d}}^{\mathrm{cf}}} \left(\sum_{m=1}^{M} \eta_{mk}^{1/2} g_{mk} \hat{g}_{mk}^* - \mathbb{E}\left\{ \sum_{m=1}^{M} \eta_{mk}^{1/2} g_{mk} \hat{g}_{mk}^* \right\} \right), \tag{21}
$$

$$
\mathrm{UI}_{kk'} \triangleq \sqrt{\rho_{\mathrm{d}}^{\mathrm{cf}}} \sum_{m=1}^{M} \eta_{mk'}^{1/2} g_{mk} \hat{g}_{mk'}^*, \tag{22}
$$

represent the strength of desired signal (DS), the beamforming gain uncertainty (BU), and the interference caused by the k'th user (UI), respectively.

We treat the sum of the second, third, and fourth terms in (19) as "effective noise". Since q_k is independent of DS_k and BU_k, we have

$$
\mathbb{E}\left\{ \mathrm{DS}_k \cdot q_k \times (\mathrm{BU}_k \cdot q_k)^* \right\} = \mathbb{E}\left\{ \mathrm{DS}_k \times \mathrm{BU}_k^* \right\} \mathbb{E}\left\{ |q_k|^2 \right\} = 0.
$$

Thus, the first and the second terms of (19) are uncorrelated. A similar calculation shows that the third and fourth terms of (19) are uncorrelated with the first term of (19). Therefore, the effective noise and the desired signal are uncorrelated. By using the fact that uncorrelated Gaussian noise represents the worst case, we obtain the following achievable rate of the kth user for Cell-Free (cf) operation:

$$
R_{\mathrm{d},k}^{\mathrm{cf}} = \log_2 \left(1 + \frac{|\mathrm{DS}_k|^2}{\mathbb{E}\{|\mathrm{BU}_k|^2\} + \sum_{k'\neq k}^{K} \mathbb{E}\{|\mathrm{UI}_{kk'}|^2\} + 1} \right). \tag{23}
$$

We next provide a new exact closed-form expression for the achievable rate (23), for a finite M.

Theorem 1: An achievable downlink rate of the transmission from the APs to the kth user in the Cell-Free Massive MIMO system with conjugate beamforming, for any finite M and K, is given by (24), shown at the top of the next page.

Proof: See Appendix A. □

Remark 3: The main differences between the capacity bound expressions for Cell-Free and collocated Massive MIMO systems [3] are: i) in Cell-Free systems, in general $\beta_{mk} \neq \beta_{m'k}$, for $m \neq m'$, whereas in collocated Massive MIMO, $\beta_{mk} = \beta_{m'k}$; and ii) in Cell-Free systems, a power constraint is applied at each AP individually, whereas in collocated systems, a total power constraint is applied at each base station. Consider the special case in which all APs are collocated and the power constraint for each AP is replaced by a total power constraint over all APs. In this case, we have $\beta_{mk} = \beta_{m'k} \triangleq \beta_k$,

$$R_{\mathrm{d},k}^{\mathrm{cf}} = \log_2\left(1 + \frac{\rho_{\mathrm{d}}^{\mathrm{cf}}\left(\sum_{m=1}^{M}\eta_{mk}^{1/2}\gamma_{mk}\right)^2}{\rho_{\mathrm{d}}^{\mathrm{cf}}\sum_{k'\neq k}^{K}\left(\sum_{m=1}^{M}\eta_{mk'}^{1/2}\gamma_{mk'}\frac{\beta_{mk}}{\beta_{mk'}}\right)^2|\boldsymbol{\varphi}_{k'}^H\boldsymbol{\varphi}_k|^2 + \rho_{\mathrm{d}}^{\mathrm{cf}}\sum_{k'=1}^{K}\sum_{m=1}^{M}\eta_{mk'}\gamma_{mk'}\beta_{mk} + 1}\right), \tag{24}$$

$$R_{\mathrm{u},k}^{\mathrm{cf}} = \log_2\left(1 + \frac{\rho_{\mathrm{u}}^{\mathrm{cf}}\eta_k\left(\sum_{m=1}^{M}\gamma_{mk}\right)^2}{\rho_{\mathrm{u}}^{\mathrm{cf}}\sum_{k'\neq k}^{K}\eta_{k'}\left(\sum_{m=1}^{M}\gamma_{mk}\frac{\beta_{mk'}}{\beta_{mk}}\right)^2|\boldsymbol{\varphi}_k^H\boldsymbol{\varphi}_{k'}|^2 + \rho_{\mathrm{u}}^{\mathrm{cf}}\sum_{k'=1}^{K}\eta_{k'}\sum_{m=1}^{M}\gamma_{mk}\beta_{mk'} + \sum_{m=1}^{M}\gamma_{mk}}\right), \tag{27}$$

$\gamma_{mk} = \gamma_{m'k} \triangleq \gamma_k$, and the power control coefficient is $\eta_{mk} = \eta_k/(M\gamma_{mk})$. If, furthermore, the K pilot sequences are pairwisely orthogonal, then, (24) becomes

$$R_{\mathrm{d},k}^{\mathrm{cf}} = \log_2\left(1 + \frac{M\rho_{\mathrm{d}}^{\mathrm{cf}}\gamma_k\eta_k}{\rho_{\mathrm{d}}^{\mathrm{cf}}\beta_k\sum_{k'=1}^{K}\eta_{k'} + 1}\right), \tag{25}$$

which is identical to the rate expression for collocated Massive MIMO systems in [3].

Remark 4: The achievable rate (24) is obtained under the assumption that the users only know the channel statistics. However, this achievable rate is close to that in the case where the users know the actual channel realizations. This is a consequence of channel hardening, as discussed in Section II. To see this more quantitatively, we compare the achievable rate (24) with the following expression,

$$\tilde{R}_{\mathrm{d},k}^{\mathrm{cf}} = \mathbb{E}\left\{\log_2\left(1 + \frac{\rho_{\mathrm{d}}^{\mathrm{cf}}\left|\sum_{m=1}^{M}\eta_{mk}^{1/2}g_{mk}\hat{g}_{mk}^*\right|^2}{\rho_{\mathrm{d}}^{\mathrm{cf}}\sum_{k'\neq k}^{K}\left|\sum_{m=1}^{M}\eta_{mk'}^{1/2}g_{mk}\hat{g}_{mk'}^*\right|^2 + 1}\right)\right\}, \tag{26}$$

which represents an achievable rate for a genie-aided user that knows the instantaneous channel gain. Figure 2 shows a comparison between (24), which assumes that the users only know the channel statistics, and the genie-aided rate (26), which assumes knowledge of the realizations. As seen in the figure, the gap is small, which means that downlink training is not necessary.

2) Achievable Uplink Rate: The central processing unit detects the desired signal q_k from $r_{\mathrm{u},k}$ in (11). We assume that the central processing unit uses only statistical knowledge of the channel when performing the detection. Using a similar methodology as in Section III-B1, we obtain a rigorous closed-form expression for the achievable uplink rate as follows.

Theorem 2: An achievable uplink rate for the kth user in the Cell-Free Massive MIMO system with matched filtering detection, for any M and K, is given by (27), shown at the top of the page.

Remark 5: In the special case that all APs are collocated and all K pilot sequences are pairwisely orthogonal, then $\beta_{mk} =$
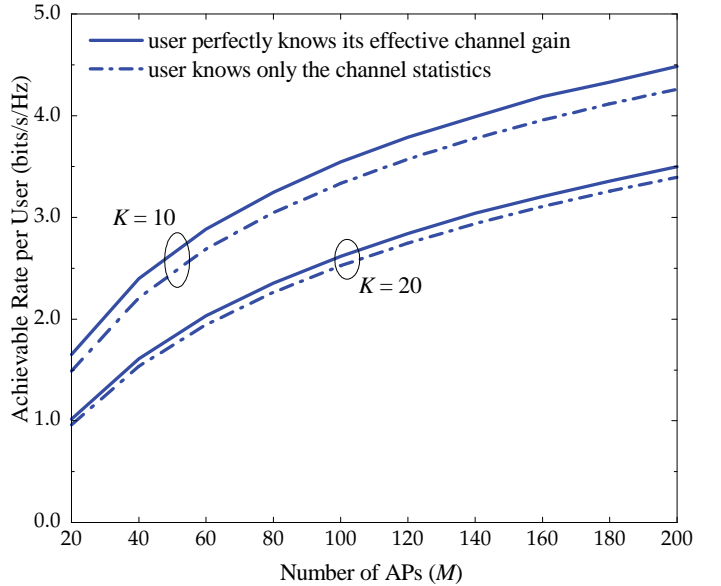

Fig. 2. The achievable rate versus the number of APs for different K. Here, $\rho_{\mathrm{d}}^{\mathrm{sc}} = 10$ dB, $\rho_{\mathrm{p}}^{\mathrm{cf}} = 0$ dB, $\tau^{\mathrm{cf}} = K$, $\beta_{mk} = 1$, $\eta_{mk} = 1/(K\gamma_{mk})$, and pilot sequences are pairwisely orthogonal.

$\beta_{m'k} \triangleq \beta_k$, $\gamma_{mk} = \gamma_{m'k} \triangleq \gamma_k$, and $\boldsymbol{\varphi}_k^H\boldsymbol{\varphi}_{k'} = 0, \forall k' \neq k$. Equation (27) then reduces to

$$R_{\mathrm{u},k}^{\mathrm{cf}} = \log_2\left(1 + \frac{M\rho_{\mathrm{u}}^{\mathrm{cf}}\eta_k\gamma_k}{\rho_{\mathrm{u}}^{\mathrm{cf}}\sum_{k'=1}^{K}\eta_{k'}\beta_{k'} + 1}\right), \tag{28}$$

which is precisely the uplink capacity lower bound of a single-cell Massive MIMO system with a collocated array obtained in [21], and a variation on that in [36].

IV. PILOT ASSIGNMENT AND POWER CONTROL

To obtain good system performance, the available radio resources must be efficiently managed. In this section, we will present methods for pilot sequence assignment and power control. Importantly, pilot assignment and power control can be performed independently, because the pilots are not power controlled.

A. Greedy Pilot Assignment

Typically, different users must use non-orthogonal pilot sequences, due to the limited length of the coherence interval.

Since the length of the pilot sequences is τ^{cf}, there exist τ^{cf} orthogonal pilot sequences. Here we focus on the case that $\tau^{\mathrm{cf}} < K$. If $\tau^{\mathrm{cf}} \geq K$, we simply assign K orthogonal pilot sequences to the K users.

A simple baseline method for assigning pilot sequences of length τ^{cf} samples to the K users is random pilot assignment [37]. With random pilot assignment, each user will be randomly assigned one pilot sequence from a predetermined set $\mathcal{S}_{\boldsymbol{\varphi}}$ of τ^{cf} orthogonal pilot sequences. Random pilot assignment could alternatively be done by letting each user choose an arbitrary unit-norm vector (i.e. not from a predetermined set of pilots). However, it appears from simulations that the latter scheme does not work well. While random pilot assignment is a useful baseline, occasionally two users in close vicinity of each other will use the same pilot sequence, which results in strong pilot contamination.

Optimal pilot assignment is a difficult combinatorial problem. We propose to use a simple greedy algorithm, which iteratively refines the pilot assignment. The K users are first randomly assigned K pilot sequences. Then the user that has the lowest downlink rate, say user k^*, updates its pilot sequence so that its pilot contamination effect is minimized.[3] The pilot contamination effect at the k^*th user is quantified by the second term in (3) which has variance

$$\mathbb{E}\left\{\left|\sum_{k' \neq k^*}^{K} g_{mk'} \boldsymbol{\varphi}_{k^*}^{H} \boldsymbol{\varphi}_{k'}\right|^2\right\} = \sum_{k' \neq k^*}^{K} \beta_{mk'} \left|\boldsymbol{\varphi}_{k^*}^{H} \boldsymbol{\varphi}_{k'}\right|^2. \quad (29)$$

The k^*th user is assigned a new pilot sequence which minimizes the pilot contamination in (29), summed over all APs:

$$\arg\min_{\boldsymbol{\varphi}_{k^*}} \sum_{m=1}^{M} \sum_{k' \neq k^*}^{K} \beta_{mk'} \left|\boldsymbol{\varphi}_{k^*}^{H} \boldsymbol{\varphi}_{k'}\right|^2$$

$$= \arg\min_{\boldsymbol{\varphi}_{k^*}} \frac{\boldsymbol{\varphi}_{k^*}^{H} \left(\sum_{m=1}^{M} \sum_{k' \neq k^*}^{K} \beta_{mk'} \boldsymbol{\varphi}_{k'} \boldsymbol{\varphi}_{k'}^{H}\right) \boldsymbol{\varphi}_{k^*}}{\boldsymbol{\varphi}_{k^*}^{H} \boldsymbol{\varphi}_{k^*}}, \quad (30)$$

where we used the fact that $\|\boldsymbol{\varphi}_{k^*}\|^2 = 1$. The algorithm then proceeds iteratively for a predetermined number of iterations.

The greedy pilot assignment algorithm can be summarized as follows.

Algorithm 1 (Greedy pilot assignment):

1) *Initialization*: choose K pilot sequences $\boldsymbol{\varphi}_1, \cdots, \boldsymbol{\varphi}_K$ using the random pilot assignment method. Choose the number of iterations, N, and set $n = 1$.
2) Compute $R_{\mathrm{d},k}^{\mathrm{cf}}$, using (24). Find the user with the lowest rate:

$$k^* = \arg\min_{k} R_{\mathrm{d},k}^{\mathrm{cf}}. \quad (31)$$

3) Update the pilot sequence for the k^*th user by choosing $\boldsymbol{\varphi}_{k^*}$ from $\mathcal{S}_{\boldsymbol{\varphi}}$ which minimizes

$$\sum_{m=1}^{M} \sum_{k' \neq k^*}^{K} \beta_{mk'} \left|\boldsymbol{\varphi}_{k^*}^{H} \boldsymbol{\varphi}_{k'}\right|^2.$$

4) Set $n := n + 1$. Stop if $n > N$. Otherwise, go to Step 2.

Remark 6: The greedy pilot assignment can be performed at the CPU, which connects to all APs via backhaul links. The pilot assignment is recomputed on the large-scale fading time scale.[4] This simplifies the signal processing at the central unit significantly. Furthermore, since $\boldsymbol{\varphi}_{k^*}$ is chosen from $\mathcal{S}_{\boldsymbol{\varphi}}$, to inform the users about their assigned pilots, the CPU only needs to send an index to each user.

B. Power Control

We next show that Cell-Free Massive MIMO can provide uniformly good service to all users, regardless of their geographical location, by using max-min power control. While power control in general is a well studied topic, the max-min power control problems that arise when optimizing Cell-Free Massive MIMO are entirely new. The power control is performed at the CPU, and importantly, is done on the large-scale fading time scale.

1) Downlink: In the downlink, given realizations of the large-scale fading, we find the power control coefficients η_{mk}, $m = 1, \cdots, M$, $k = 1, \cdots, K$, that maximize the minimum of the downlink rates of all users, under the power constraint (7). At the optimum point, all users get the same rate. Mathematically:

$$\begin{aligned} \max_{\{\eta_{mk}\}} \quad & \min_{k=1,\cdots,K} R_{\mathrm{d},k}^{\mathrm{cf}} \\ \text{subject to} \quad & \sum_{k=1}^{K} \eta_{mk} \gamma_{mk} \leq 1, \ m = 1, ..., M \\ & \eta_{mk} \geq 0, \ k = 1, ..., K, \ m = 1, ..., M, \end{aligned} \quad (32)$$

where $R_{\mathrm{d},k}^{\mathrm{cf}}$ is given by (24). Define $\varsigma_{mk} \triangleq \eta_{mk}^{1/2}$. Then, from (24), (32) is equivalent to

$$\begin{aligned} \max_{\{\eta_{mk}\}} \quad & \min_{k=1,\cdots,K} \frac{\left(\sum_{m=1}^{M} \gamma_{mk} \varsigma_{mk}\right)^2}{\sum_{k' \neq k}^{K} \xi_{kk'} \left(\sum_{m=1}^{M} \frac{\gamma_{mk'} \beta_{mk} \varsigma_{mk'}}{\beta_{mk'}}\right)^2 + \sum_{m=1}^{M} \beta_{mk} \sum_{k'=1}^{K} \gamma_{mk'} \varsigma_{mk'}^2 + \frac{1}{\rho_{\mathrm{d}}^{\mathrm{cf}}}} \\ \text{s.t.} \quad & \sum_{k=1}^{K} \eta_{mk} \gamma_{mk} \leq 1, \ m = 1, ..., M \\ & \eta_{mk} \geq 0, \ k = 1, ..., K, \ m = 1, ..., M, \end{aligned}$$

$$(33)$$

where $\xi_{kk'} \triangleq |\boldsymbol{\varphi}_{k'}^{H} \boldsymbol{\varphi}_k|^2$.

---

[3]In principle, this "worst user" could be taken to be the user that has either the lowest uplink or the lowest downlink rate. In our numerical experiments, we reassign the pilot of the user having the lowest downlink rate, hence giving downlink performance some priority over uplink performance.

[4]Hence this recomputation is infrequent even in high mobility. For example, at user mobility of $v = 100$ km/h, and a carrier frequency of $f_{\mathrm{c}} = 2$ GHz, the channel coherence time is on the order of a millisecond. The large-scale fading changes much more slowly, at least some 40 times slower according to [29], [30]. As a result, the greedy pilot assignment method must only be done a few times per second.

By introducing slack variables $\varrho_{k'k}$ and ϑ_m, we reformulate (33) as follows:

$$
\max_{\{\varsigma_{mk},\varrho_{k'k},\vartheta_m\}} \min_{k=1,\cdots,K} \frac{\left(\sum_{m=1}^{M} \gamma_{mk}\varsigma_{mk}\right)^2}{\sum_{k'\neq k}^{K} |\boldsymbol{\varphi}_{k'}^H \boldsymbol{\varphi}_k|^2 \varrho_{k'k}^2 + \sum_{m=1}^{M} \beta_{mk}\vartheta_m^2 + \frac{1}{\rho_{\mathrm{d}}^{\mathrm{cf}}}}
$$

$$
\begin{aligned}
\text{subject to} \quad & \sum_{k'=1}^{K} \gamma_{mk'}\varsigma_{mk'}^2 \leq \vartheta_m^2, \ m=1,...,M \\
& \sum_{m=1}^{M} \gamma_{mk'} \frac{\beta_{mk}}{\beta_{mk'}} \varsigma_{mk'} \leq \varrho_{k'k}, \ \forall k' \neq k \\
& 0 \leq \vartheta_m \leq 1, \ m=1,...,M \\
& \varsigma_{mk} \geq 0, \ k=1,...,K, \ m=1,...,M.
\end{aligned}
\tag{34}
$$

The equivalence between (33) and (34) follows directly from the fact that the first and second constraints in (34) hold with equality at the optimum.

Proposition 1: The objective function of (34) is quasi-concave, and the problem (34) is quasi-concave.

Proof: See Appendix B. $\qquad\square$

Consequently, (34) can be solved efficiently by a bisection search, in each step solving a sequence of convex feasibility problem [38]. Specifically, the following algorithm solves (34).

Algorithm 2 (Bisection algorithm for solving (34)):

1) *Initialization*: choose the initial values of $t_{\min}$ and $t_{\max}$, where $t_{\min}$ and $t_{\max}$ define a range of relevant values of the objective function in (34). Choose a tolerance $\epsilon > 0$.

2) Set $t := \frac{t_{\min}+t_{\max}}{2}$. Solve the following convex feasibility program:

$$
\begin{cases}
\|\mathbf{v}_k\| \leq \frac{1}{\sqrt{t}} \sum_{m=1}^{M} \gamma_{mk}\varsigma_{mk}, \ k=1,...,K, \\
\sum_{k'=1}^{K} \gamma_{mk'}\varsigma_{mk'}^2 \leq \vartheta_m^2, \ m=1,...,M, \\
\sum_{m=1}^{M} \gamma_{mk'} \frac{\beta_{mk}}{\beta_{mk'}} \varsigma_{mk'} \leq \varrho_{k'k}, \ \forall k' \neq k, \\
0 \leq \vartheta_m \leq 1, \ m=1,...,M, \\
\varsigma_{mk} \geq 0, \ k=1,...,K, \ m=1,...,M,
\end{cases}
\tag{35}
$$

where $\mathbf{v}_k \triangleq \left[\mathbf{v}_{k1}^T \mathbf{I}_{-k} \ \ \mathbf{v}_{k2}^T \ \ \frac{1}{\sqrt{\rho_{\mathrm{d}}^{\mathrm{cf}}}}\right]^T$, and where $\mathbf{v}_{k1} \triangleq \left[\boldsymbol{\varphi}_1^H \boldsymbol{\varphi}_k \varrho_{1k} \ ... \ \boldsymbol{\varphi}_K^H \boldsymbol{\varphi}_K \varrho_{Kk}\right]^T$, $\mathbf{I}_{-k}$ is a $K \times (K-1)$ matrix obtained from the $K \times K$ identity matrix with the kth column removed, and $\mathbf{v}_{k2} \triangleq \left[\sqrt{\beta_{1k}}\vartheta_1 \ ... \ \sqrt{\beta_{Mk}}\vartheta_M\right]^T$.

3) If problem (35) is feasible, then set $t_{\min} := t$, else set $t_{\max} := t$.

4) Stop if $t_{\max} - t_{\min} < \epsilon$. Otherwise, go to Step 2.

Remark 7: The max-min power control problem can be directly extended to a max-min weighted rate problem, where the K users are weighted according to priority: $\max \min\{w_k R_k\}$, where $w_k > 0$ is the weighting factor of the kth user. A user with higher priority will be assigned a smaller weighting factor.

2) Uplink: In the uplink, the max-min power control problem can be formulated as follows:

$$
\begin{aligned}
\max_{\{\eta_k\}} \quad & \min_{k=1,\cdots,K} R_{\mathrm{u},k}^{\mathrm{cf}} \\
\text{subject to} \quad & 0 \leq \eta_k \leq 1, \ k=1,...,K,
\end{aligned}
\tag{36}
$$

where $R_{\mathrm{u},k}^{\mathrm{cf}}$ is given by (27). Problem (36) can be equivalently reformulated as

$$
\begin{aligned}
\max_{\{\eta_k\},t} \quad & t \\
\text{subject to} \quad & t \leq R_{\mathrm{u},k}^{\mathrm{cf}}, \ k=1,...,K \\
& 0 \leq \eta_k \leq 1, \ k=1,...,K.
\end{aligned}
\tag{37}
$$

Proposition 2: The optimization problem (37) is quasi-linear.

Proof: From (27), for a given t, all inequalities involved in (37) are linear, and hence, the program (37) is quasi-linear. $\qquad\square$

Consequently, Problem (37) can be efficiently solved by using bisection and solving a sequence of linear feasibility problems.

V. SMALL-CELL SYSTEM

In this section, we give the system model, achievable rate expressions, and max-min power control for small-cell systems. These will be used in Section VI where we compare the performance of Cell-Free Massive MIMO and small-cell systems.

For small-cell systems, we assume that each user is served by only one AP. For each user, the available AP with the largest average received useful signal power is selected. If an AP has already been chosen by another user, this AP becomes unavailable. The AP selection is done user by user in a random order. Let m_k be the AP chosen by the kth user. Then,

$$
m_k \triangleq \arg\max_{m\in\{\text{available APs}\}} \beta_{mk}.
\tag{38}
$$

We consider a short enough time scale that handovers between APs do not occur. This modeling choice was made to enable a rigorous performance analysis. While there is precedent for this assumption in other literature [12], [39], future work may address the issue of handovers. As a result of this assumption, the performance figures we obtain for small-cell systems may be overoptimistic.

In contrast to Cell-Massive MIMO, in the small-cell systems, the channel does not harden. Specifically, while in Cell-Free Massive MIMO the effective channel is an inner product between two M-vectors—hence close to its mean, in the small-cell case the effective channel is a single Rayleigh fading scalar coefficient. Consequently, both the users and the APs must estimate their effective channel gain in order to demodulate the symbols, which requires both uplink and downlink training. The detailed transmission protocols for the uplink and downlink of small-cell systems are as follows.

A. Downlink Transmission

In the downlink, the users first estimate their channels based on pilots sent from the APs. The so-obtained channel estimates are used to detect the desired signals.

Let $\tau_{\mathrm{d}}^{\mathrm{sc}}$ be the downlink training duration in samples, $\sqrt{\tau_{\mathrm{d}}^{\mathrm{sc}}}\boldsymbol{\phi}_k \in \mathbb{C}^{\tau_{\mathrm{d}}^{\mathrm{sc}}\times 1}$, where $\|\boldsymbol{\phi}_k\|^2 = 1$, is the pilot sequence transmitted from the m_kth AP, and $\rho_{\mathrm{d,p}}^{\mathrm{sc}}$ is the transmit power per downlink pilot symbol. The MMSE estimate of $g_{m_k k}$ can be expressed as

$$
\hat{g}_{m_k k} = g_{m_k k} - \varepsilon_{m_k k},
\tag{39}
$$

$$R_{\mathrm{d},k}^{\mathrm{sc}} = \mathbb{E}\left\{\log_2\left(1 + \frac{\rho_{\mathrm{d}}^{\mathrm{sc}}\alpha_{\mathrm{d},k}\,|\hat{g}_{m_k k}|^2}{\rho_{\mathrm{d}}^{\mathrm{sc}}\alpha_{\mathrm{d},k}(\beta_{m_k k} - \mu_{m_k k}) + \rho_{\mathrm{d}}^{\mathrm{sc}}\sum_{k'\neq k}^{K}\alpha_{\mathrm{d},k'}\beta_{m_{k'}k} + 1}\right)\right\}, \tag{42}$$

where $\varepsilon_{m_k k}$ is the channel estimation error, which is independent of the channel estimate $\hat{g}_{m_k k}$. Furthermore, we have $\hat{g}_{m_k k} \sim \mathcal{CN}\left(0, \mu_{m_k k}\right)$ and $\varepsilon_{m_k k} \sim \mathcal{CN}\left(0, \beta_{m_k k} - \mu_{m_k k}\right)$, where

$$\mu_{m_k k} \triangleq \frac{\tau_{\mathrm{d}}^{\mathrm{sc}}\rho_{\mathrm{d,p}}^{\mathrm{sc}}\beta_{m_k k}^2}{\tau_{\mathrm{d}}^{\mathrm{sc}}\rho_{\mathrm{d,p}}^{\mathrm{sc}}\sum_{k'=1}^{K}\beta_{m_{k'}k}\left|\boldsymbol{\phi}_k^H\boldsymbol{\phi}_{k'}\right|^2 + 1}. \tag{40}$$

After sending the pilots for the channel estimation, the K chosen APs send the data. Let $\sqrt{\alpha_{\mathrm{d},k}}q_k$, $\mathbb{E}\left\{|q_k|^2\right\} = 1$, be the symbol transmitted from the m_kth AP, destined for the kth user, where $\alpha_{\mathrm{d},k}$ is a power control coefficient, $0 \le \alpha_{\mathrm{d},k} \le 1$. The kth user receives

$$\begin{aligned}
y_k &= \sqrt{\rho_{\mathrm{d}}^{\mathrm{sc}}}\sum_{k'=1}^{K}g_{m_{k'}k}\sqrt{\alpha_{\mathrm{d},k'}}q_{k'} + w_k \\
&= \sqrt{\rho_{\mathrm{d}}^{\mathrm{sc}}}\hat{g}_{m_k k}\sqrt{\alpha_{\mathrm{d},k}}q_k + \sqrt{\rho_{\mathrm{d}}^{\mathrm{sc}}}\varepsilon_{m_k k}\sqrt{\alpha_{\mathrm{d},k}}q_k \\
&\quad + \sqrt{\rho_{\mathrm{d}}^{\mathrm{sc}}}\sum_{k'\neq k}^{K}g_{m_{k'}k}\sqrt{\alpha_{\mathrm{d},k'}}q_{k'} + w_k,
\end{aligned} \tag{41}$$

where $\rho_{\mathrm{d}}^{\mathrm{sc}}$ is the normalized downlink transmit SNR and $w_k \sim \mathcal{CN}\left(0, 1\right)$ is additive Gaussian noise.

Remark 8: In small-cell systems, since only one single-antenna AP is involved in transmission to a given user, the concept of "conjugate beamforming" becomes void. Downlink transmission entails only transmitting the symbol destined for the kth user, appropriately scaled to meet the transmit power constraint. Channel estimation at the user is required in order to demodulate, as there is no channel hardening (see discussion above).

1) Achievable Downlink Rate: Treating the last three terms of (41) as uncorrelated effective noise, we obtain the achievable downlink rate for the kth user as in (42), shown at the top of the page.

Since the channel does not harden, applying the bounding techniques in Section III, while not impossible in principle, would yield very pessimistic capacity bounds. However, since $|\hat{g}_{m_k k}|^2$ is exponentially distributed with mean $\mu_{m_k k}$, the achievable rate in (42) can be expressed in closed form in terms of the exponential integral function $\mathrm{Ei}(\cdot)$ [40, Eq. (8.211.1)] as:

$$R_{\mathrm{d},k}^{\mathrm{sc}} = -(\log_2 e)e^{1/\bar{\mu}_{m_k k}}\mathrm{Ei}\left(-\frac{1}{\bar{\mu}_{m_k k}}\right), \tag{43}$$

where

$$\bar{\mu}_{m_k k} \triangleq \frac{\rho_{\mathrm{d}}^{\mathrm{sc}}\alpha_{\mathrm{d},k}\mu_{m_k k}}{\rho_{\mathrm{d}}^{\mathrm{sc}}\alpha_{\mathrm{d},k}(\beta_{m_k k} - \mu_{m_k k}) + \rho_{\mathrm{d}}^{\mathrm{sc}}\sum_{k'\neq k}^{K}\alpha_{\mathrm{d},k'}\beta_{m_{k'}k} + 1}. \tag{44}$$

2) Max-Min Power Control: As in the Cell-Free Massive MIMO systems, we consider max-min power control which can be formulated as follows:

$$\begin{aligned}
\max_{\{\alpha_{\mathrm{d},k}\}} \quad & \min_{k=1,\cdots,K} R_{\mathrm{d},k}^{\mathrm{sc}} \\
\text{subject to} \quad & 0 \le \alpha_{\mathrm{d},k} \le 1, \; k = 1,\cdots,K.
\end{aligned} \tag{45}$$

Since $R_{\mathrm{d},k}^{\mathrm{sc}}$ is a monotonically increasing function of $\bar{\mu}_{m_k k}$, (45) is equivalent to

$$\begin{aligned}
\max_{\{\alpha_{\mathrm{d},k}\}} \quad & \min_{k=1,\cdots,K} \bar{\mu}_{m_k k} \\
\text{subject to} \quad & 0 \le \alpha_{\mathrm{d},k} \le 1, \; k = 1,\cdots,K.
\end{aligned} \tag{46}$$

Problem (46) is a quasi-linear program, which can be solved by using bisection.

B. Uplink Transmission

In the uplink, the APs first estimate the channels based on pilots sent from the users. The so-obtained channel estimates are used to detect the desired signals. Let $\rho_{\mathrm{u}}^{\mathrm{sc}}$ and $0 \le \alpha_{\mathrm{u},k} \le 1$ be the normalized SNR and the power control coefficient at the kth user, respectively. Then, following the same methodology as in the derivation of the downlink transmission, we obtain the following achievable uplink rate for the kth user:

$$R_{\mathrm{u},k}^{\mathrm{sc}} = -(\log_2 e)e^{1/\bar{\omega}_{m_k k}}\mathrm{Ei}\left(-\frac{1}{\bar{\omega}_{m_k k}}\right), \tag{47}$$

where

$$\bar{\omega}_{m_k k} \triangleq \frac{\rho_{\mathrm{u}}^{\mathrm{sc}}\alpha_{\mathrm{u},k}\omega_{m_k k}}{\rho_{\mathrm{u}}^{\mathrm{sc}}\alpha_{\mathrm{u},k}(\beta_{m_k k} - \omega_{m_k k}) + \rho_{\mathrm{u}}^{\mathrm{sc}}\sum_{k'\neq k}^{K}\alpha_{\mathrm{u},k'}\beta_{m_k k'} + 1}, \tag{48}$$

and where $\omega_{m_k k}$ is given by

$$\omega_{m_k k} \triangleq \frac{\tau_{\mathrm{u}}^{\mathrm{sc}}\rho_{\mathrm{u,p}}^{\mathrm{sc}}\beta_{m_k k}^2}{\tau_{\mathrm{u}}^{\mathrm{sc}}\rho_{\mathrm{u,p}}^{\mathrm{sc}}\sum_{k'=1}^{K}\beta_{m_k k'}\left|\boldsymbol{\psi}_k^H\boldsymbol{\psi}_{k'}\right|^2 + 1}. \tag{49}$$

In (49), $\tau_{\mathrm{u}}^{\mathrm{sc}}$ is the uplink training duration in samples, $\sqrt{\tau_{\mathrm{u}}^{\mathrm{sc}}}\boldsymbol{\psi}_k \in \mathbb{C}^{\tau_{\mathrm{u}}^{\mathrm{sc}} \times 1}$, where $\|\boldsymbol{\psi}_k\|^2 = 1$, is the pilot sequence transmitted from the kth user, and $\rho_{\mathrm{u,p}}^{\mathrm{sc}}$ is the transmit power per uplink pilot symbol.

Similarly to in the downlink, the max-min power control problem for the uplink can be formulated as a quasi-linear program:

$$\begin{aligned}
\max_{\{\alpha_{\mathrm{u},k}\}} \quad & \min_{k=1,\cdots,K} \bar{\omega}_{m_k k} \\
\text{subject to} \quad & 0 \le \alpha_{\mathrm{u},k} \le 1, \; k = 1,\cdots,K,
\end{aligned} \tag{50}$$

which can be solved by using bisection.

VI. NUMERICAL RESULTS AND DISCUSSIONS

We quantitatively study the performance of Cell-Free Massive MIMO, and compare it to that of small-cell systems. We specifically demonstrate the effects of shadow fading correlation. The M APs and K users are uniformly distributed at random within a square of size $D \times D$ km^2.

A. Large-Scale Fading Model

We describe the path loss and shadow fading correlation models, which are used in the performance evaluation. The large-scale fading coefficient β_{mk} in (1) models the path loss and shadow fading, according to

$$\beta_{mk} = \text{PL}_{mk} \cdot 10^{\frac{\sigma_{\text{sh}} z_{mk}}{10}}, \tag{51}$$

where PL_{mk} represents the path loss, and $10^{\frac{\sigma_{\text{sh}} z_{mk}}{10}}$ represents the shadow fading with the standard deviation σ_{sh}, and $z_{mk} \sim \mathcal{N}(0,1)$.

1) Path loss Model: We use a three-slope model for the path loss [41]: the path loss exponent equals 3.5 if distance between the mth AP and the kth user (denoted by d_{mk}) is greater than d_1, equals 2 if $d_1 \geq d_{mk} > d_0$, and equals 0 if $d_{mk} \leq d_0$ for some d_0 and d_1. When $d_{mk} > d_1$, we employ the Hata-COST231 propagation model. More precisely, the path loss in dB is given by

$$\text{PL}_{mk} = \begin{cases} -L - 35\log_{10}(d_{mk}), & \text{if } d_{mk} > d_1 \\ -L - 15\log_{10}(d_1) - 20\log_{10}(d_{mk}), & \text{if } d_0 < d_{mk} \leq d_1 \\ -L - 15\log_{10}(d_1) - 20\log_{10}(d_0), & \text{if } d_{mk} \leq d_0 \end{cases} \tag{52}$$

where

$$L \triangleq 46.3 + 33.9\log_{10}(f) - 13.82\log_{10}(h_{\text{AP}}) \\ - (1.1\log_{10}(f) - 0.7)h_{\text{u}} + (1.56\log_{10}(f) - 0.8), \tag{53}$$

and where f is the carrier frequency (in MHz), h_{AP} is the AP antenna height (in m), and h_{u} denotes the user antenna height (in m). The path loss PL_{mk} is a continuous function of d_{mk}. Note that when $d_{mk} \leq d_1$, there is no shadowing.

2) Shadowing Correlation Model: Most previous work assumed that the shadowing coefficients (and therefore z_{mk}) are uncorrelated. However, in practice, transmitters/receivers that are in close vicinity of each other may be surrounded by common obstacles, and hence, the shadowing coefficients are correlated. This correlation may significantly affect the system performance.

For the shadow fading coefficients, we will use a model with two components [42]:

$$z_{mk} = \sqrt{\delta}a_m + \sqrt{1-\delta}b_k, \quad m = 1,\ldots,M, \ K = 1,\ldots,K, \tag{54}$$

where $a_m \sim \mathcal{N}(0,1)$ and $b_k \sim \mathcal{N}(0,1)$ are independent random variables, and δ, $0 \leq \delta \leq 1$, is a parameter. The variable a_m models contributions to the shadow fading that result from obstructing objects in the vicinity of the mth AP, and which affects the channel from that AP to all users in the same way. The variable b_k models contributions to the shadow fading that result from objects in the vicinity of the kth user, and which affects the channels from that user to all APs in the same way. When $\delta = 0$, the shadow fading from a given

user is the same to all APs, but different users are affected by different shadow fading. Conversely, when $\delta = 1$, the shadow fading from a given AP is the same to all users; however, different APs are affected by different shadow fading. Varying δ between 0 and 1 trades off between these two extremes.

The covariance functions of a_m and b_k are given by:

$$\mathbb{E}\{a_m a_{m'}\} = 2^{-\frac{d_{\text{a}}(m,m')}{d_{\text{decorr}}}}, \quad \mathbb{E}\{b_k b_{k'}\} = 2^{-\frac{d_{\text{u}}(k,k')}{d_{\text{decorr}}}}, \tag{55}$$

where $d_{\text{a}}(m,m')$ is the geographical distance between the mth and m'th APs, $d_{\text{u}}(k,k')$ is the geographical distance between the kth and k'th users, and d_{decorr} is a decorrelation distance which depends on the environment. Typically, the decorrelation distance is on the order of 20ÂŬ–200 m. A shorter decorrelation distance corresponds to an environment with a lower degree of stationarity. This model for correlation between different geographical locations has been validated both in theory and by practical experiments [42], [43].

B. Parameters and Setup

In all examples, we choose the parameters summarized in Table I. The quantities $\bar{\rho}_{\text{d}}^{\text{cf}}$, $\bar{\rho}_{\text{u}}^{\text{cf}}$, and $\bar{\rho}_{\text{p}}^{\text{cf}}$ in this table are the transmit powers of downlink data, uplink data, and pilot symbols, respectively. The corresponding normalized transmit SNRs $\rho_{\text{d}}^{\text{cf}}$, $\rho_{\text{u}}^{\text{cf}}$, and $\rho_{\text{p}}^{\text{cf}}$ can be computed by dividing these powers by the noise power, where the noise power is given by

$$\text{noise power} = \text{bandwidth} \times k_{\text{B}} \times T_0 \times \text{noise figure (W)},$$

where $k_{\text{B}} = 1.381 \times 10^{-23}$ (Joule per Kelvin) is the Boltzmann constant, and $T_0 = 290$ (Kelvin) is the noise temperature. To avoid boundary effects, and to imitate a network with an infinite area, the square area is wrapped around at the edges, and hence, the simulation area has eight neighbors.

We consider the per-user net throughputs which take into account the channel estimation overhead, and are defined as follows:

$$S_{\text{A},k}^{\text{cf}} = B \frac{1 - \tau^{\text{cf}}/\tau_{\text{c}}}{2} R_{\text{A},k}^{\text{cf}}, \tag{56}$$

$$S_{\text{A},k}^{\text{sc}} = B \frac{1 - (\tau_{\text{d}}^{\text{sc}} + \tau_{\text{u}}^{\text{sc}})/\tau_{\text{c}}}{2} R_{\text{A},k}^{\text{sc}}, \tag{57}$$

where $\text{A} \in \{\text{d}, \text{u}\}$ correspond to downlink respectively uplink transmission, B is the spectral bandwidth, and τ_{c} is again the coherence interval in samples. The terms $\tau^{\text{cf}}/\tau_{\text{c}}$ and $(\tau_{\text{d}}^{\text{sc}} + \tau_{\text{u}}^{\text{sc}})/\tau_{\text{c}}$ in (56) and (57) reflect the fact that, for each coherence interval of length τ_{c} samples, in the Cell-Free Massive MIMO systems, we spend τ^{cf} samples for the uplink training, while

TABLE I
SYSTEM PARAMETERS FOR THE SIMULATION.

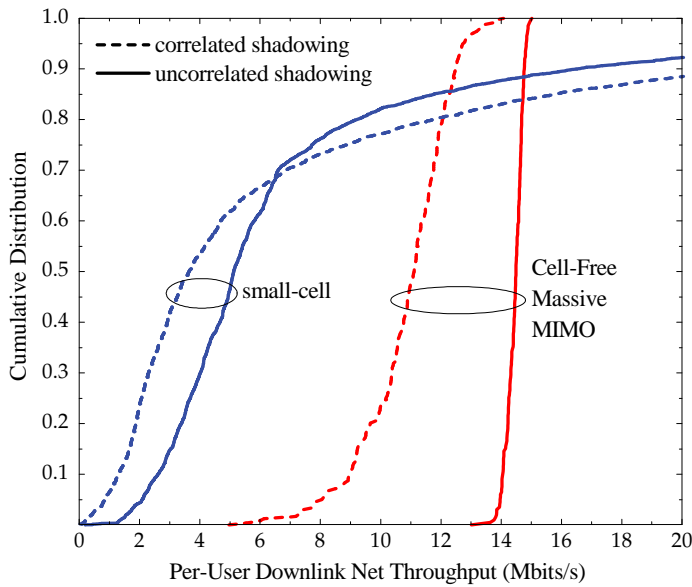| Parameter	Value
Carrier frequency	1.9 GHz
Bandwidth	20 MHz
Noise figure (uplink and downlink)	9 dB
AP antenna height	15 m
User antenna height	1.65 m
$\bar{\rho}_{\text{d}}^{\text{cf}}, \bar{\rho}_{\text{u}}^{\text{cf}}, \bar{\rho}_{\text{p}}^{\text{cf}}$	200, 100, 100 mW
σ_{sh}	8 dB
D, d_1, d_0	1000, 50, 10 m

Fig. 3. The cumulative distribution of the per-user downlink net throughput for correlated and uncorrelated shadow fading, with the greedy pilot assignment and max-min power control. Here, $M = 100$, $K = 40$, and $\tau^{\mathrm{cf}} = \tau^{\mathrm{sc}}_{\mathrm{d}} = 20$.
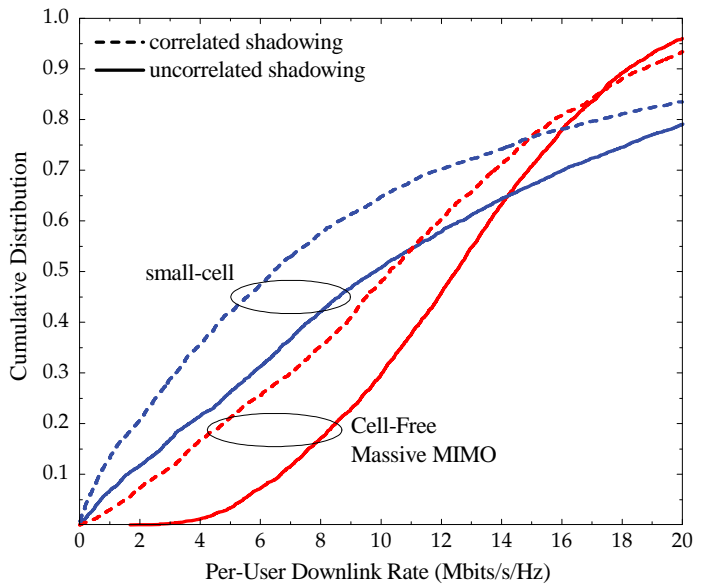
Fig. 5. The cumulative distribution of the per-user downlink net throughput for correlated and uncorrelated shadow fading, with the greedy pilot assignment and without power control. Here, $M = 100$, $K = 40$, and $\tau^{\mathrm{cf}} = \tau^{\mathrm{sc}}_{\mathrm{d}} = 20$.
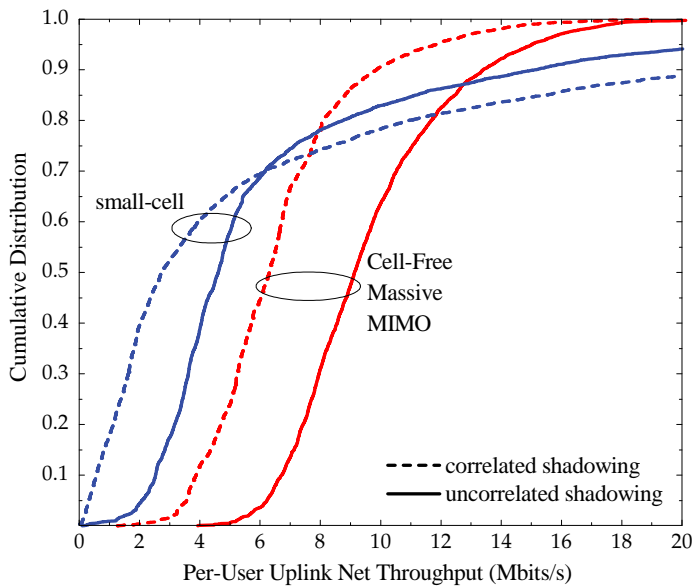

Fig. 4. The same as Figure 3 but for the uplink, and $\tau^{\mathrm{cf}} = \tau^{\mathrm{sc}}_{\mathrm{u}} = 20$.
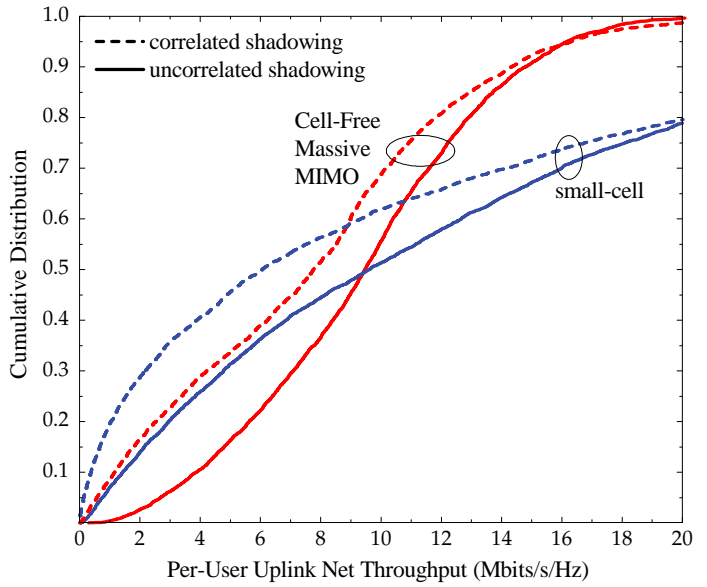

Fig. 6. The same as Figure 5 but for the uplink, and $\tau^{\mathrm{cf}} = \tau^{\mathrm{sc}}_{\mathrm{u}} = 20$.

in the small-cell systems, we spend $\tau^{\mathrm{sc}}_{\mathrm{d}} + \tau^{\mathrm{sc}}_{\mathrm{u}}$ samples for the uplink and downlink training. In all examples, we take $\tau_{\mathrm{c}} = 200$ samples, corresponding to a coherence bandwidth of 200 KHz and a coherence time of 1 ms, and choose $B = 20$ MHz.

To ensure a fair comparison between Cell-Free Massive MIMO and small-cell systems, we choose $\rho^{\mathrm{sc}}_{\mathrm{d}} = \frac{M}{K}\rho^{\mathrm{cf}}_{\mathrm{d}}$, $\rho^{\mathrm{sc}}_{\mathrm{u}} = \rho^{\mathrm{cf}}_{\mathrm{u}}$, and $\rho^{\mathrm{sc}}_{\mathrm{u,p}} = \rho^{\mathrm{sc}}_{\mathrm{d,p}} = \rho^{\mathrm{cf}}_{\mathrm{p}}$, which makes the total radiated power equal in all cases. The cumulative distributions of the per-user downlink/uplink net throughput in our examples are generated as follows:

- For the case with max-min power control: 1) 200 random realizations of the AP/user locations and shadow fading

profiles are generated; 2) for each realization, the per-user net throughputs of K users are computed by using max-min power control as discussed in Section IV-B for Cell-Free Massive MIMO and in Section V for small-cell systems—with max-min power control these throughputs are the same for all users; 3) a cumulative distribution is generated over the so-obtained per-user net throughputs.

- For the case without power control: same procedure, but in 2) no power control is performed. Without power control, for Cell-Free Massive MIMO, in the downlink transmission, all APs transmit with full power, and at the mth AP, the power control coefficients η_{mk}, $k = 1, \ldots K$, are the same, i.e., $\eta_{mk} = \left(\sum_{k'=1}^{K} \gamma_{mk'} \right)^{-1}$,
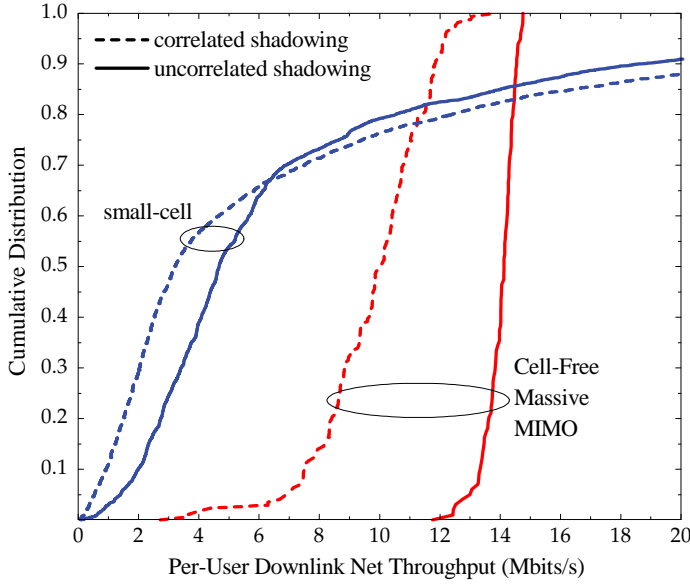
Fig. 7. The cumulative distribution of the per-user downlink net throughput for correlated and uncorrelated shadow fading, with the random pilot assignment and max-min power control. Here, $M = 100$, $K = 40$, and $\tau^{\mathrm{cf}} = \tau_{\mathrm{d}}^{\mathrm{sc}} = 20$.

Fig. 8. The same as Figure 7 but for the uplink, and $\tau^{\mathrm{cf}} = \tau_{\mathrm{u}}^{\mathrm{sc}} = 20$.

$\forall k = 1, \ldots K$, (this directly comes from (7)), while in the uplink, all users transmit with full power, i.e., $\eta_k = 1$, $\forall k = 1, \ldots K$. For the small-cell system, in the downlink, all chosen APs transmit with full power, i.e. $\alpha_{\mathrm{d},k} = 1$, and in the uplink, all users transmit with full power, i.e. $\alpha_{\mathrm{u},k} = 1$, $k = 1, \ldots K$.

- For the correlated shadow fading scenario, we use the shadowing correlation model discussed in Section VI-A2, and we choose $d_{\mathrm{decorr}} = 0.1$ km and $\delta = 0.5$.
- For the small-cell systems, the greedy pilot assignment works in the same way as the scheme for Cell-Free Massive MIMO discussed in Section IV-A, except for that in the small-cell systems, since the chosen APs do not cooperate, the worst user will find a new pilot which minimizes the pilot contamination corresponding to its AP (rather than summed over all APs as in the case of Cell-Free systems).

Fig. 9. Cumulative distribution of the effective number of APs serving each user. Here, $M = 100$, $K = 40$, and $\tau^{\mathrm{cf}} = 5$ and 20.

C. Results and Discussions

We first compare the performance of Cell-Free Massive MIMO with that of small-cell systems with greedy pilot assignment and max-min power control. Figure 3 compares the cumulative distribution of the per-user downlink net throughput for Cell-Free Massive MIMO and small-cell systems, with $M = 100$, $K = 40$, and $\tau^{\mathrm{cf}} = \tau_{\mathrm{d}}^{\mathrm{sc}} = \tau_{\mathrm{u}}^{\mathrm{sc}} = 20$, with and without shadow fading correlation.

Cell-Free Massive MIMO significantly outperforms small-cell in both median and in 95%-likely performance. The net throughput of Cell-Free Massive MIMO is much more concentrated around its median, compared with the small-cell systems. Without shadow fading correlation, the 95%-likely net throughput of the Cell-Free downlink is about 14 Mbits/s which is 7 times higher than that of the small-cell downlink
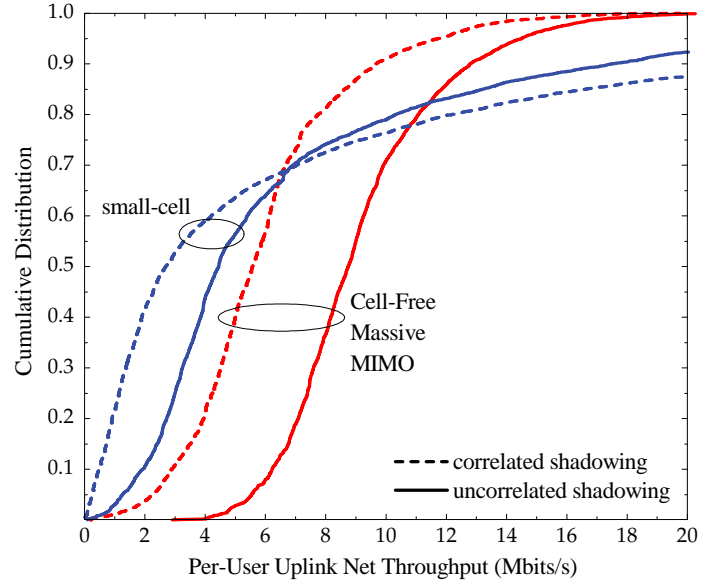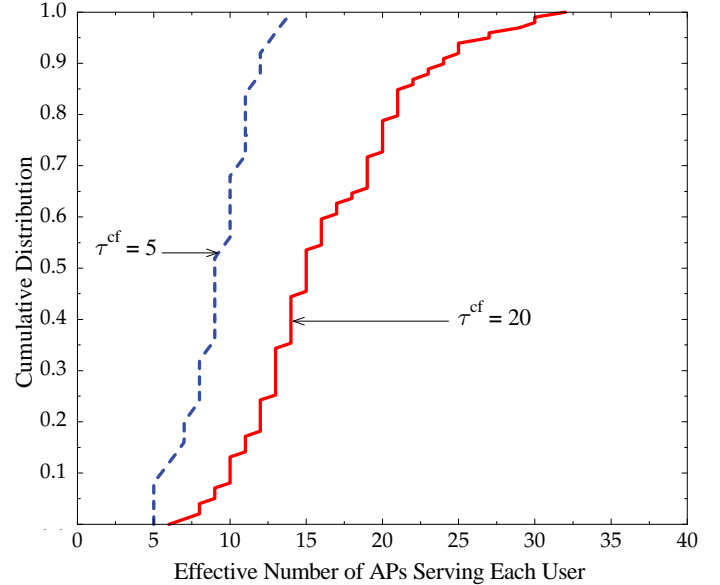
(about 2.1 Mbits/s). In particular, we can see that the small-cell systems are much more affected by shadow fading correlation than Cell-Free Massive MIMO is. This is due to the fact that when the shadowing coefficients are highly correlated, the gain from choosing the best APs in a small-cell system is reduced. With shadowing correlation, the 95%-likely net throughput of the Cell-Free downlink is about 10 times higher than that of the small-cell system. The same insights can be obtained for the uplink, see Figure 4. In addition, owing to the fact that the downlink uses more power (since $M > K$ and $\rho_{\mathrm{d}}^{\mathrm{cf}} > \rho_{\mathrm{u}}^{\mathrm{cf}}$) and has more power control coefficients to choose than the uplink does, the downlink performance is better than the uplink performance.

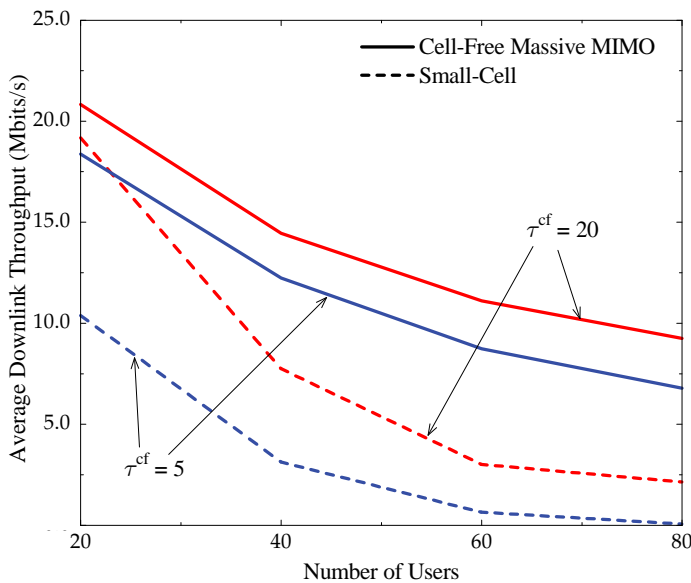Next we compare Cell-Free Massive MIMO and small-cell

Fig. 10. The average downlink net throughput versus the number of users for different τ^{cf}. Here, $M = 100$.

Fig. 11. The average downlink net throughput versus the number of APs for different τ^{cf}. Here, $K = 20$.

systems, assuming that no power control is performed. Figures 5 and 6 show the cumulative distributions of the per-user net throughput for the downlink and the uplink, respectively, with $M = 100$, $K = 40$, and $\tau^{\mathrm{cf}} = \tau_{\mathrm{d}}^{\mathrm{sc}} = \tau_{\mathrm{u}}^{\mathrm{sc}} = 20$, and with the greedy pilot assignment method. In both uncorrelated and correlated shadowing scenarios, Cell-Free Massive MIMO outperforms the small-cell approach in terms of 95%-likely per-user net throughput. In addition, a comparison of Figure 3 (or 4) and Figure 5 (or 6) shows that with power control, the performance of Cell-Free Massive MIMO improves significantly in terms of both median and 95%-likely throughput. In the uncorrelated shadow fading scenario, the power allocation can improve the 95%-likely Cell-Free throughput by a factor of 2.5 for the downlink and a factor of 2.3 for the uplink, compared with the case without power control. For the small-cell system, power control improves the 95%-likely throughput but not the median throughput (recall that the power control policy explicitly aims at improving the performance of the worst user).

In Figures 7 and 8, we consider the same setting as in Figures 3 and 4, but here we use the random pilot assignment scheme. These figures provide the same insights as Figures 3 and 4. Furthermore, by comparing these figures with Figures 3 and 4, we can see that with greedy pilot assignment, the 95%-likely net throughputs can be improved by about 20% compared with when random pilot assignment is used.

In addition, we study how the M APs assign powers to a given user in the downlink of Cell-Free Massive MIMO. From (5), the average transmit power expended by the mth AP on the kth user is $\rho_{\mathrm{d}}^{\mathrm{cf}} \eta_{mk} \gamma_{mk}$. Then

$$p(m, k) \triangleq \frac{\eta_{mk} \gamma_{mk}}{\sum_{m'=1}^{M} \eta_{m'k} \gamma_{m'k}} \qquad (58)$$

is the ratio between the power spent by the mth AP on the kth user and the total power collectively spent by all APs on the kth user. Figure 9 shows the cumulative distribution of
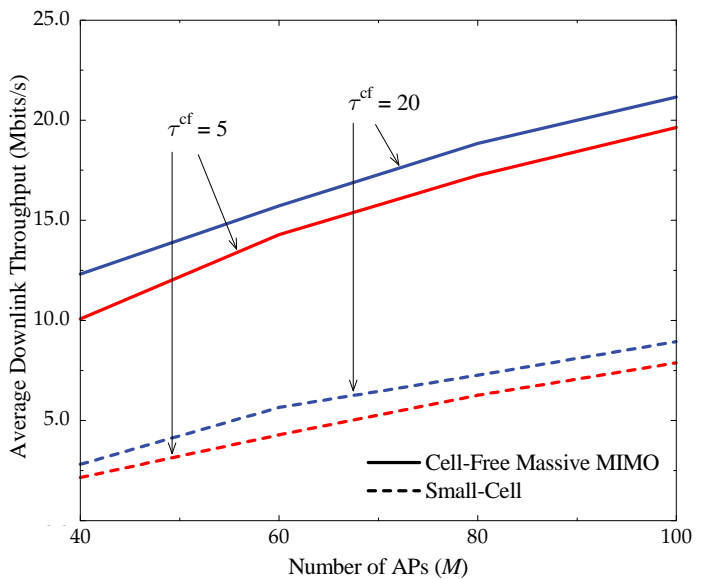
the effective number of APs serving each user, for $\tau^{\mathrm{cf}} = 5$ and 20, and uncorrelated shadow fading. The effective number of APs serving each user is defined as the minimum number of APs that contribute at least 95% of the power allocated to a given user. This plot was generated as follows: 1) 200 random realizations of the AP/user locations and shadow fading profiles were generated, each with $M = 100$ APs and $K = 40$ users; 2) for each user k in each realization, we found the minimum number of APs, say n, such that the n largest values of $\{p(m, k)\}$ sum up to at least 95% (k is arbitrary here, since all users have the same statistics); 3) a cumulative distribution was generated over the 200 realizations. We can see that, on average, only about 10–20 of the 100 APs really participate in serving a given user. The larger τ^{cf}, the less pilot contamination and the more accurate channel estimates— hence, more AP points can usefully serve each user.

Finally, we investigate the effect of the number of users K, number of APs M, and the training duration τ^{cf} on the performance of Cell-Free Massive MIMO and small-cell systems. Figure 10 shows the average downlink net throughput versus K for different τ^{cf}, at $M = 100$ and uncorrelated shadow fading. The average is taken over the large-scale fading. We can see that when reducing K or τ^{cf}, the effect of pilot contamination increases, and hence, the performance decreases. As expected, Cell-Free Massive MIMO systems outperform small-cell systems. Cell-Free Massive MIMO benefits from favorable propagation, and therefore, it suffers less from interference than the small-cell system does. As a result, for a fixed τ^{cf}, the relative performance gap between Cell-Free Massive MIMO and small-cell systems increases with K. Figure 11 shows the average downlink net throughput versus M for different τ^{cf}, at $K = 20$. Owing to the array gain (for Cell-Free Massive MIMO systems) and diversity gain (for small-cell systems), the system performances of both Cell-Free Massive MIMO and small-cell systems increase when M

increases. Again, for all M, Cell-Free Massive MIMO systems are significantly better than small-cell systems.

Tables II and III summarize the downlink respectively uplink performances of the Cell-Free Massive MIMO and small-cell systems, under uncorrelated and correlated shadow fading.

VII. CONCLUSION

We analyzed the performance of Cell-Free Massive MIMO, taking into account the effects of channel estimation, non-orthogonality of pilot sequences, and power control. A comparison between Cell-Free Massive MIMO systems and small-cell systems was also performed, under uncorrelated and correlated shadow fading.

The results show that Cell-Free Massive MIMO systems can significantly outperform small-cell systems in terms of throughput. In particular, Cell-Free systems are much more robust to shadow fading correlation than small-cell systems. The 95%-likely per-user throughputs of Cell-Free Massive MIMO with shadowing correlation are an order of magnitude higher than those of the small-cell systems. In terms of implementation complexity, however, small-cell systems require much less backhaul than Cell-Free Massive MIMO.

APPENDIX

A. Proof of Theorem 1

To derive the closed-form expression for the achievable rate given in (23), we need to compute $\mathtt{DS}_k$, $\mathbb{E}\left\{|\mathtt{BU}_k|^2\right\}$, and $\mathbb{E}\left\{|\mathtt{UI}_{kk'}|^2\right\}$.

1) Compute $\mathtt{DS}_k$: Let $\varepsilon_{mk} \triangleq g_{mk} - \hat{g}_{mk}$ be the channel estimation error. Owing to the properties of MMSE estimation, ε_{mk} and $\hat{g}_{mk}$ are independent. Thus, we have

$$\mathtt{DS}_k = \sqrt{\rho_{\mathrm{d}}^{\mathrm{cf}}}\, \mathbb{E}\left\{\sum_{m=1}^{M} \eta_{mk}^{1/2}(\hat{g}_{mk} + \varepsilon_{mk})\hat{g}_{mk}^*\right\}$$
$$= \sqrt{\rho_{\mathrm{d}}^{\mathrm{cf}}} \sum_{m=1}^{M} \eta_{mk}^{1/2}\gamma_{mk}. \tag{59}$$

2) Compute $\mathbb{E}\left\{|\mathtt{BU}_k|^2\right\}$: Since the variance of a sum of independent RVs is equal to the sum of the variances, we have

$$\mathbb{E}\left\{|\mathtt{BU}_k|^2\right\} = \rho_{\mathrm{d}}^{\mathrm{cf}} \sum_{m=1}^{M} \eta_{mk}\, \mathbb{E}\left\{\left|g_{mk}\hat{g}_{mk}^* - \mathbb{E}\left\{g_{mk}\hat{g}_{mk}^*\right\}\right|^2\right\}$$
$$= \rho_{\mathrm{d}}^{\mathrm{cf}} \sum_{m=1}^{M} \eta_{mk}\left(\mathbb{E}\left\{|g_{mk}\hat{g}_{mk}^*|^2\right\} - |\mathbb{E}\left\{g_{mk}\hat{g}_{mk}^*\right\}|^2\right)$$
$$= \rho_{\mathrm{d}}^{\mathrm{cf}} \sum_{m=1}^{M} \eta_{mk}\left(\mathbb{E}\left\{\left|\varepsilon_{mk}\hat{g}_{mk}^* + |\hat{g}_{mk}|^2\right|^2\right\} - \gamma_{mk}^2\right)$$
$$\overset{(a)}{=} \rho_{\mathrm{d}}^{\mathrm{cf}} \sum_{m=1}^{M} \eta_{mk}\left(\mathbb{E}\left\{|\varepsilon_{mk}\hat{g}_{mk}^*|^2\right\} + \mathbb{E}\left\{|\hat{g}_{mk}|^4\right\} - \gamma_{mk}^2\right)$$
$$\overset{(b)}{=} \rho_{\mathrm{d}}^{\mathrm{cf}} \sum_{m=1}^{M} \eta_{mk}\left(\gamma_{mk}(\beta_{mk} - \gamma_{mk}) + 2\gamma_{mk}^2 - \gamma_{mk}^2\right)$$
$$= \rho_{\mathrm{d}}^{\mathrm{cf}} \sum_{m=1}^{M} \eta_{mk}\gamma_{mk}\beta_{mk}, \tag{60}$$

where (a) follows that fact that ε_{mk} has zero mean and is independent of $\hat{g}_{mk}$, while (b) follows from the facts that $\mathbb{E}\left\{|\hat{g}_{mk}|^4\right\} = 2\gamma_{mk}^2$ and $\mathbb{E}\left\{|\varepsilon_{mk}|^2\right\} = \beta_{mk} - \gamma_{mk}$.

3) Compute $\mathbb{E}\left\{|\mathtt{UI}_{kk'}|^2\right\}$: From (4) and (22), we have

$$\mathbb{E}\left\{|\mathtt{UI}_{k'}|^2\right\} = \rho_{\mathrm{d}}^{\mathrm{cf}}\, \mathbb{E}\left\{\left|\sum_{m=1}^{M} \eta_{mk'}^{1/2} c_{mk'} g_{mk}\right.\right.$$
$$\left.\left. \times \left(\sqrt{\tau^{\mathrm{cf}}\rho_{\mathrm{p}}^{\mathrm{cf}}} \sum_{i=1}^{K} g_{mi}\boldsymbol{\varphi}_{k'}^H\boldsymbol{\varphi}_i + \tilde{w}_{mk'}\right)^*\right|^2\right\}, \tag{61}$$

TABLE II

THE 95%-LIKELY PER-USER NET THROUGHPUT (MBITS/S) OF THE CELL-FREE AND SMALL-CELL DOWNLINK, FOR $M = 100$, $K = 40$, AND $\tau^{\mathrm{cf}} = \tau_{\mathrm{d}}^{\mathrm{sc}} = 20$.

	greedy pilot assignment with power control		greedy pilot assignment without power control		random pilot assignment with power control	
	uncorrelated shadowing	correlated shadowing	uncorrelated shadowing	correlated shadowing	uncorrelated shadowing	correlated shadowing
Cell-Free	14	8.12	5.46	1.58	12.70	6.95
Small-cell	2.08	0.83	0.86	0.24	1.37	0.54

TABLE III

THE 95%-LIKELY PER-USER NET THROUGHPUT (MBITS/S) OF THE CELL-FREE AND SMALL-CELL UPLINK, FOR $M = 100$, $K = 40$, AND $\tau^{\mathrm{cf}} = \tau_{\mathrm{u}}^{\mathrm{sc}} = 20$.

	greedy pilot assignment with power control		greedy pilot assignment without power control		random pilot assignment with power control	
	uncorrelated shadowing	correlated shadowing	uncorrelated shadowing	correlated shadowing	uncorrelated shadowing	correlated shadowing
Cell-Free	6.29	3.55	2.71	0.56	5.54	2.26
Small-cell	2.04	0.31	0.76	0.13	1.27	0.26

where $\tilde{w}_{mk'} \triangleq \boldsymbol{\varphi}_{k'}^H \mathbf{w}_{\mathrm{p},m} \sim \mathcal{CN}(0,1)$. Since $\tilde{w}_{mk'}$ is independent of g_{mi}, $\forall i, k'$, we have

$$
\begin{aligned}
\mathbb{E}\left\{|\mathtt{UI}_{kk'}|^2\right\} &= \rho_{\mathrm{d}}^{\mathrm{cf}} \, \mathbb{E}\left\{\left|\sum_{m=1}^{M} \eta_{mk'}^{1/2} c_{mk'} g_{mk} \tilde{w}_{mk'}^*\right|^2\right\} \\
&+ \tau^{\mathrm{cf}} \rho_{\mathrm{p}}^{\mathrm{cf}} \rho_{\mathrm{d}}^{\mathrm{cf}} \, \mathbb{E}\left\{\left|\sum_{m=1}^{M} \eta_{mk'}^{1/2} c_{mk'} g_{mk} \left(\sum_{i=1}^{K} g_{mi} \boldsymbol{\varphi}_{k'}^H \boldsymbol{\varphi}_i\right)^*\right|^2\right\}.
\end{aligned}
\tag{62}
$$

Using the fact that if X and Y are two independent RVs and $\mathbb{E}\{X\} = 0$, then $\mathbb{E}\left\{|X+Y|^2\right\} = \mathbb{E}\left\{|X|^2\right\} + \mathbb{E}\left\{|Y|^2\right\}$, (62) can be rewritten as follows

$$
\mathbb{E}\left\{|\mathtt{UI}_{kk'}|^2\right\} = \rho_{\mathrm{d}}^{\mathrm{cf}} \sum_{m=1}^{M} \eta_{mk'} c_{mk'}^2 \beta_{mk} + \tau^{\mathrm{cf}} \rho_{\mathrm{p}}^{\mathrm{cf}} \rho_{\mathrm{d}}^{\mathrm{cf}} (\mathcal{T}_1 + \mathcal{T}_2),
\tag{63}
$$

where

$$
\mathcal{T}_1 \triangleq \mathbb{E}\left\{\left|\sum_{m=1}^{M} \eta_{mk'}^{1/2} c_{mk'} |g_{mk}|^2 \boldsymbol{\varphi}_{k'}^H \boldsymbol{\varphi}_k\right|^2\right\},
\tag{64}
$$

$$
\mathcal{T}_2 \triangleq \mathbb{E}\left\{\left|\sum_{m=1}^{M} \eta_{mk'}^{1/2} c_{mk'} g_{mk} \left(\sum_{i \neq k}^{K} g_{mi} \boldsymbol{\varphi}_{k'}^H \boldsymbol{\varphi}_i\right)^*\right|^2\right\}.
\tag{65}
$$

We first compute $\mathcal{T}_1$. We have

$$
\begin{aligned}
\mathcal{T}_1 &= \left|\boldsymbol{\varphi}_{k'}^H \boldsymbol{\varphi}_k\right|^2 \mathbb{E}\left\{\sum_{m=1}^{M}\sum_{n=1}^{M} \eta_{mk'}^{1/2} \eta_{nk'}^{1/2} c_{mk'} c_{nk'} |g_{mk}|^2 |g_{nk}|^2\right\} \\
&= \left|\boldsymbol{\varphi}_{k'}^H \boldsymbol{\varphi}_k\right|^2 \mathbb{E}\left\{\sum_{m=1}^{M} \eta_{mk'} c_{mk'}^2 |g_{mk}|^4\right\} \\
&+ \left|\boldsymbol{\varphi}_{k'}^H \boldsymbol{\varphi}_k\right|^2 \mathbb{E}\left\{\sum_{m=1}^{M}\sum_{n \neq m}^{M} \eta_{mk'}^{1/2} \eta_{nk'}^{1/2} c_{mk'} c_{nk'} |g_{mk}|^2 |g_{nk}|^2\right\} \\
&= 2\left|\boldsymbol{\varphi}_{k'}^H \boldsymbol{\varphi}_k\right|^2 \sum_{m=1}^{M} \eta_{mk'} c_{mk'}^2 \beta_{mk}^2 \\
&+ \left|\boldsymbol{\varphi}_{k'}^H \boldsymbol{\varphi}_k\right|^2 \sum_{m=1}^{M}\sum_{n \neq m}^{M} \eta_{mk'}^{1/2} \eta_{nk'}^{1/2} c_{mk'} c_{nk'} \beta_{mk} \beta_{nk}.
\end{aligned}
\tag{66}
$$

Similarly, we have

$$
\mathcal{T}_2 = \sum_{m=1}^{M}\sum_{i \neq k}^{K} \eta_{mk'} c_{mk'}^2 \beta_{mk} \beta_{mi} \left|\boldsymbol{\varphi}_{k'}^H \boldsymbol{\varphi}_i\right|^2.
\tag{67}
$$

Substitution of (66) and (67) into (63) yields

$$
\begin{aligned}
\mathbb{E}\left\{|\mathtt{UI}_{kk'}|^2\right\} &= \rho_{\mathrm{d}}^{\mathrm{cf}} \left|\boldsymbol{\varphi}_{k'}^H \boldsymbol{\varphi}_k\right|^2 \left(\sum_{m=1}^{M} \eta_{mk'}^{1/2} \gamma_{mk'} \frac{\beta_{mk}}{\beta_{mk'}}\right)^2 \\
&+ \rho_{\mathrm{d}}^{\mathrm{cf}} \sum_{m=1}^{M} \eta_{mk'} \gamma_{mk'} \beta_{mk}.
\end{aligned}
\tag{68}
$$

Plugging (59), (60), and (68) into (23), we obtain (24).

B. Proof of Proposition 1

Denote by $\mathcal{S} \triangleq \{\varsigma_{mk}, \varrho_{k'k}, \vartheta_m\}$ the set of variables, and $f(\mathcal{S})$ the objective function of (34):

$$
f(\mathcal{S}) \triangleq \min_{k=1,\cdots,K} \frac{\left(\sum_{m=1}^{M} \gamma_{mk} \varsigma_{mk}\right)^2}{\sum_{k' \neq k}^{K} |\boldsymbol{\varphi}_{k'}^H \boldsymbol{\varphi}_k|^2 \varrho_{k'k}^2 + \sum_{m=1}^{M} \beta_{mk} \vartheta_m^2 + \frac{1}{\rho_{\mathrm{d}}^{\mathrm{cf}}}}.
\tag{69}
$$

For any $t \in \mathbb{R}_+$, the upper-level set of $f(\mathcal{S})$ that belongs to $\mathcal{S}$ is

$$
\begin{aligned}
U(f,t) &= \{\mathcal{S} : f(\mathcal{S}) \geq t\} \\
&= \left\{\mathcal{S} : \frac{\left(\sum_{m=1}^{M} \gamma_{mk} \varsigma_{mk}\right)^2}{\sum_{k' \neq k}^{K} |\boldsymbol{\varphi}_{k'}^H \boldsymbol{\varphi}_k|^2 \varrho_{k'k}^2 + \sum_{m=1}^{M} \beta_{mk} \vartheta_m^2 + \frac{1}{\rho_{\mathrm{d}}^{\mathrm{cf}}}} \geq t, \forall k\right\} \\
&= \left\{\mathcal{S} : \|\mathbf{v}_k\| \leq \frac{1}{\sqrt{t}} \sum_{m=1}^{M} \gamma_{mk} \varsigma_{mk}, \forall k\right\},
\end{aligned}
\tag{70}
$$

where $\mathbf{v}_k \triangleq \begin{bmatrix} \mathbf{v}_{k1}^T \mathbf{I}_{-k} & \mathbf{v}_{k2}^T & \frac{1}{\sqrt{\rho_{\mathrm{d}}^{\mathrm{cf}}}} \end{bmatrix}^T$, and where $\mathbf{v}_{k1} \triangleq \begin{bmatrix} \boldsymbol{\varphi}_1^H \boldsymbol{\varphi}_k \varrho_{1k} & \cdots & \boldsymbol{\varphi}_K^H \boldsymbol{\varphi}_K \varrho_{Kk} \end{bmatrix}^T$, $\mathbf{I}_{-k}$ is a $K \times (K-1)$ matrix obtained from the $K \times K$ identity matrix with the kth column is removed, and $\mathbf{v}_{k2} \triangleq \begin{bmatrix} \sqrt{\beta_{1k}} \vartheta_1 & \cdots & \sqrt{\beta_{Mk}} \vartheta_M \end{bmatrix}^T$.

Since the upper-level set $U(f,t)$ can be represented as a SOC, it is a convex set. Thus, $f(\mathcal{S})$ is quasi-concave. Furthermore, the optimization problem (34) is a quasi-concave optimization problem since the constraint set in (34) is also convex.

REFERENCES

[1] H. Q. Ngo, A. Ashikhmin, H. Yang, E. G. Larsson, and T. L. Marzetta, "Cell-free massive MIMO: Uniformly great service for everyone," in *Proc. IEEE International Workshop on Signal Processing Advances in Wireless Communications (SPAWC)*, Stockholm, Sweden, Jun. 2015.

[2] T. L. Marzetta, "Noncooperative cellular wireless with unlimited numbers of base station antennas," *IEEE Trans. Wireless Commun.*, vol. 9, no. 11, pp. 3590–3600, Nov. 2010.

[3] H. Yang and T. L. Marzetta, "A macro cellular wireless network with uniformly high user throughputs," in *Proc. IEEE Veh. Technol. Conf. (VTC)*, Sep. 2014.

[4] S. Zhou, M. Zhao, X. Xu, J. Wang, and Y. Yao, "Distributed wireless communication system: A new architecture for future public wireless access," *IEEE Commun. Mag.*, vol. 41, no. 3, pp. 108–113, Mar. 2003.

[5] T. L. Marzetta, E. G. Larsson, H. Yang, and H. Q. Ngo, *Fundamentals of Massive MIMO*. Cambridge, UK: Cambridge University Press, 2016.

[6] M. Karakayali, G. Foschini, and R. Valenzuela, "Network coordination for spectrally efficient communications in cellular systems," *IEEE Wireless Commun. Mag.*, vol. 13, no. 4, pp. 56–61, Aug. 2006.

[7] W. Choi and J. Andrews, "Downlink performance and capacity of distributed antenna systems in a multicell environment," *IEEE Trans. Wireless Commun.*, vol. 6, no. 1, pp. 69–73, Jan. 2007.

[8] R. Irmer, H. Droste, P. Marsch, M. Grieger, G. Fettweis, S. Brueck, H. P. Mayer, L. Thiele, and V. Jungnickel, "Coordinated multipoint: Concepts, performance, and field trial results," *IEEE Commun. Mag.*, vol. 49, no. 2, pp. 102–111, Feb. 2011.

[9] X. Hong, Y. Jie, C.-X. Wang, J. Shi, and X. Ge, "Energy-spectral efficiency trade-off in virtual MIMO cellular systems," *IEEE J. Sel. Areas Commun.*, vol. 31, no. 10, pp. 2128–2140, Oct. 2013.

[10] D. Castanheira and A. Gameiro, "Distributed antenna system capacity scaling," *IEEE Wireless Commun. Mag.*, vol. 17, no. 3, pp. 68–75, Jun. 2010.

[11] R. Heath, S. Peters, Y. Wang, and J. Zhang, "A current per spective on distributed antenna systems for the downlink of cellular systems," *IEEE Commun. Mag.*, vol. 51, no. 4, pp. 161–167, Apr. 2013.

[12] Z. Liu and L. Dai, "A comparative study of downlink MIMO cellular networks with co-located and distributed base-station antennas," *IEEE Trans. Wireless Commun.*, vol. 13, no. 11, pp. 6259–6274, Nov. 2014.

[13] Q. Sun, S. Jin, J. Wang, Y. Zhang, X. Gao, and K. K. Wong, "On scheduling for massive distributed MIMO downlink," in *Proc. IEEE Global Communications Conf. (GLOBECOM)*, GA, USA, Dec. 2013, pp. 4151–4156.

[14] M. Matthaiou, C. Zhong, M. R. McKay, and T. Ratnarajah, "Sum rate analysis of ZF receivers in distributed MIMO systems," *IEEE J. Sel. Areas Commun.*, vol. 31, no. 2, pp. 180–191, Feb. 2013.

[15] K. Hosseini, W. Yu, and R. S. Adve, "Large-scale MIMO versus network MIMO for multicell interference mitigation," *IEEE J. Select. Topics Signal Process.*, vol. 8, no. 5, pp. 930–941, Oct. 2014.

[16] J. Joung, Y. K. Chia, and S. Sun, "Energy-efficient, large-scale distributed-antenna system (L-DAS) for multiple users," *IEEE J. Select. Topics Signal Process.*, vol. 8, no. 5, pp. 930–941, Oct. 2014.

[17] Q. Ye, O. Y. Bursalioglu, and H. C. Papadopoulos, "Harmonized cellular and distributed massive MIMO: Load balancing and scheduling," in *Proc. IEEE Global Communications Conf. (GLOBECOM)*, CA, USA, Dec. 2015.

[18] J. Wang and L. Dai, "Asymptotic rate analysis of downlink multi-user systems with co-located and distributed antennas," *IEEE Trans. Wireless Commun.*, vol. 14, no. 6, pp. 3046–3058, Jun. 2015.

[19] A. Lozano, R. W. Heath, Jr., and J. G. Andrews, "Fundamental limits of cooperations," *IEEE Trans. Inf. Theory*, vol. 59, no. 1, pp. 5213–5226, Sep. 2013.

[20] H. Yin, D. Gesbert, and L. Cottatellucci, "Dealing with interference in distributed large-scale MIMO systems: A statistical approach," *IEEE J. Select. Topics Signal Process.*, vol. 8, no. 5, pp. 942–953, Oct. 2014.

[21] H. Yang and T. L. Marzetta, "Capacity performance of multicell large scale antenna systems," in *Proc. 51st Allerton Conference on Communication, Control, and Computing*, Urbana-Champaign, Illinois, Oct. 2013.

[22] K. T. Truong and R. W. Heath Jr., "The viability of distributed antennas for massive MIMO systems," in *Proc. 45th Asilomar Conference on Signals, Systems and Computers (ACSSC)*, Pacific Grove, CA, USA, Nov. 2013, pp. 1318–1323.

[23] E. Nayebi, A. Ashikhmin, T. L. Marzetta, and H. Yang, "Cell-free massive MIMO systems," in *Proc. 49th Asilomar Conference on Signals, Systems and Computers (ACSSC)*, Pacific Grove, CA, USA, Nov. 2015.

[24] H. Huh, A. M. Tulino, and G. Caire, "Network MIMO with linear zero-forcing beamforming: Large system analysis, impact of channel estimation, and reduced-complexity scheduling," *IEEE Trans. Inf. Theory*, vol. 58, no. 5, pp. 2911–2934, May 2012.

[25] W. Liu, S. Han, and C. Yang, "Energy efficiency comparison of massive MIMO and small cell network," in *Proc. IEEE Global Conference on Signal and Information Processing (GlobalSIP)*, Atlanta, GA, Dec. 2014, pp. 617–621.

[26] E. Björnson, L. Sanguinetti, and M. Kountouris, "Deploying dense networks for maximal energy efficiency: Small cells meet massive MIMO," *IEEE J. Sel. Areas Commun.*, vol. 34, no. 4, pp. 832–847, Apr. 2016.

[27] H. S. Dhillon, M. Kountouris, and J. G. Andrews, "Downlink MIMO HetNets: Modeling, ordering results and performance analysis," *IEEE Trans. Wireless Commun.*, vol. 12, no. 10, pp. 5208–5222, Oct. 2013.

[28] L. W. A. He, M. Elkashlan, Y. Chen, and K. K. Wong, "Spectrum and energy efficiency in massive mimo enabled HetNets: A stochastic geometry approach," *IEEE Commun. Lett.*, vol. 19, no. 12, pp. 2294–2297, Dec. 2015.

[29] T. S. Rappaport, *Wireless communications: principles and practice*. NJ: Prentice-Hall: Upper Saddle River, 1956.

[30] A. Ashikhmin, T. L. Marzetta, and L. Li, "Interference reduction in multi-cell massive MIMO systems I: Large-scale fading precoding and decoding," *IEEE Trans. Inf. Theory*, Nov. 2014, submitted.

[31] F. Kaltenberger, J. Haiyong, M. Guillaud, and R. Knopp, "Relative channel reciprocity calibration in MIMO/TDD systems," in *Proc. Future Network and Mobile Summit*, Florence, Italy, Jun. 2010.

[32] P. Marsch and G. Fettweis, "Uplink CoMP under a constrained backhaul and imperfect channel knowledge," *IEEE Trans. Wireless Commun.*, vol. 10, no. 6, pp. 1730–1742, Jun. 2011.

[33] O. Simeone, O. Somekh, E. Erkip, H. Poor, and S. Shamai, "A broadcast approach to robust communications over unreliable

[34] H. Cramer, *Random Variables and Probability Distributions*. Cambridge, UK: Cambridge University Press, 1970.

[35] B. Hassibi and B. M. Hochwald, "How much training is needed in multiple-antenna wireless links?" *IEEE Trans. Inf. Theory*, vol. 49, no. 4, pp. 951–963, Apr. 2003.

[36] H. Q. Ngo, E. G. Larsson, and T. L. Marzetta, "Energy and spectral efficiency of very large multiuser MIMO systems," *IEEE Trans. Commun.*, vol. 61, no. 4, pp. 1436–1449, Apr. 2013.

[37] H. Ahmadi, A. Farhang, N. Marchetti, and A. MacKenzie, "A game theoretical approach for pilot contamination avoidance in massive MIMO," *IEEE Wireless Commun. Lett.*, Oct. 2015, to appear.

[38] S. Boyd and L. Vandenberghe, *Convex Optimization*. Cambridge, UK: Cambridge University Press, 2004.

[39] J. G. Andrews, F. Baccelli, and R. K. Ganti, "A tractable approach to coverage and rate in cellular networks," *IEEE Trans. Commun.*, vol. 59, no. 11, pp. 3122–3134, Nov. 2011.

[40] I. S. Gradshteyn and I. M. Ryzhik, *Table of Integrals, Series, and Products*, 7th ed. San Diego, CA: Academic, 2007.

[41] A. Tang, J. Sun, and K. Gong, "Mobile propagation loss with a low base station antenna for NLOS street microcells in urban area," in *Proc. IEEE Veh. Technol. Conf. (VTC)*, May 2001, pp. 333–336.

[42] Z. Wang, E. K. Tameh, and A. R. Nix, "Joint shadowing process in urban peer-to-peer radio channels," *IEEE Trans. Veh. Technol.*, vol. 57, no. 1, pp. 52–64, Jan. 2008.

[43] M. Gudmundson, "Correlation model for shadow fading in mobile radio systems," *Electon. Lett.*, vol. 27, no. 23, pp. 2145–2146, Nov. 1991.

multi-relay networks," in *Proc. Information Theory and Applications Workshop (ITW)*, Taormina, Italy, Feb. 2009.

Hien Quoc Ngo received the B.S. degree in electrical engineering from Ho Chi Minh City University of Technology, Vietnam, in 2007. He then received the M.S. degree in Electronics and Radio Engineering from Kyung Hee University, Korea, in 2010, and the Ph.D. degree in communication systems from Linköping University (LiU), Sweden, in 2015. From May to December 2014, he visited Bell Laboratories, Murray Hill, New Jersey, USA.

Hien Quoc Ngo is currently a postdoctoral researcher of the Division for Communication Systems in the Department of Electrical Engineering (ISY) at Linköping University, Sweden. He is also a Visiting Research Fellow at the School of Electronics, Electrical Engineering and Computer Science, Queen's University Belfast, U.K. His current research interests include massive (large-scale) MIMO systems and cooperative communications.

Dr. Hien Quoc Ngo received the IEEE ComSoc Stephen O. Rice Prize in Communications Theory in 2015. He also received the IEEE Sweden VT-COM-IT Joint Chapter Best Student Journal Paper Award in 2015. He was an *IEEE Communications Letters* exemplary reviewer for 2014, an *IEEE Transactions on Communications* exemplary reviewer for 2015. He has been a member of Technical Program Committees for several IEEE conferences such as ICC, Globecom, WCNC, VTC, WCSP, ISWCS, ATC, ComManTel.

Alexei Ashikhmin is a Distinguished Member of Technical Staff in the Communications and Statistical Sciences Research Department of Bell Labs, Murray Hill, New Jersey. His research interests include communications theory, massive MIMO, classical and quantum information theory, and error correcting codes.

In 2014 Dr. Ashikhmin received Thomas Edison Patent Award for Patent on Massive MIMO System with Decentralized Antennas. In 2004 he received the Stephen O. Rice Prize for the best paper of IEEE Transactions on Communications. In 2002, 2010, and 2011 he received Bell Laboratories President Awards for breakthrough research in communication projects.

From 2003 to 2006, and 2011 to 2014 Dr. Ashikhmin served as an Associate Editor for IEEE Transactions on Information Theory.

Hong Yang is a member of technical staff at Nokia Bell Labs' Mathematics of Networks and Communications Research Department in Murray Hill, New Jersey, where he conducts research in communications networks. He has previously worked in both the Systems Engineering Department and the Wireless Design Center at Lucent and Alcatel-Lucent, and for a start-up network technology company. He has co-authored many research papers in wireless communications, applied mathematics, and financial economics, co-invented many U.S. and international patents, and co-authored a book Fundamentals of Massive MIMO (Cambridge, 2016). He received his Ph.D. in applied mathematics from Princeton University, Princeton, New Jersey.

Erik G. Larsson is Professor of Communication Systems at Linköping University (LiU) in Linköping, Sweden. He previously worked for the Royal Institute of Technology (KTH) in Stockholm, Sweden, the University of Florida, USA, the George Washington University, USA, and Ericsson Research, Sweden. In 2015 he was a Visiting Fellow at Princeton University, USA, for four months. He received his Ph.D. degree from Uppsala University, Sweden, in 2002.

His main professional interests are within the areas of wireless communications and signal processing. He has co-authored some 130 journal papers on these topics, he is co-author of the two Cambridge University Press textbooks *Space-Time Block Coding for Wireless Communications* (2003) and *Fundamentals of Massive MIMO* (2016). He is co-inventor on 16 issued and many pending patents on wireless technology.

He served as Associate Editor for, among others, the *IEEE Transactions on Communications* (2010-2014) and *IEEE Transactions on Signal Processing* (2006-2010). During 2015–2016 he served as chair of the IEEE Signal Processing Society SPCOM technical committee, and in 2017 he is the past chair of this committee. He served chair of the steering committee for the *IEEE Wireless Communications Letters* in 2014–2015. He was the General Chair of the Asilomar Conference on Signals, Systems and Computers in 2015, and Technical Chair in 2012. He is a member of the IEEE Signal Processing Society Awards Board during 2017–2019.

He received the *IEEE Signal Processing Magazine* Best Column Award twice, in 2012 and 2014, and the IEEE ComSoc Stephen O. Rice Prize in Communications Theory in 2015. He is a Fellow of the IEEE.

Thomas L. Marzetta was born in Washington, D.C. He received the PhD and SB in Electrical Engineering from Massachusetts Institute of Technology in 1978 and 1972, and the MS in Systems Engineering from University of Pennsylvania in 1973. After careers in petroleum exploration at Schlumberger-Doll Research and defense research at Nichols Research Corporation, he joined Bell Labs in 1995 where he is currently a Bell Labs Fellow. Previously he directed the Communications and Statistical Sciences Department within the former Mathematical Sciences Research Center.

Dr. Marzetta is on the Advisory Board of MAMMOET (Massive MIMO for Efficient Transmission), an EU-sponsored FP7 project, and he was Coordinator of the GreenTouch Consortium's Large Scale Antenna Systems Project. He has received awards including the 2015 IEEE Stephen O. Rice Prize, the 2015 IEEE W. R. G. Baker Award, and the 2013 IEEE Guglielmo Marconi Prize Paper Award. He was elected a Fellow of the IEEE in 2003, and he received an Honorary Doctorate from Linköping University in 2015.